[American Journal of Science, Vol. 315, October, 2015, P. 734–780, DOI 10.2475/08.2015.02]

A GENERALIZED MODEL FOR PREDICTING THE THERMODYNAMIC PROPERTIES OF CLAY MINERALS

PHILIPPE BLANC*,†, PHILIPPE VIEILLARD**, HÉLÈNE GAILHANOU*, STÉPHANE GABOREAU*, ÉRIC GAUCHER*, CLAIRE I. FIALIPS§, BENOÎT MADÉ§, and ERIC GIFFAUT§

ABSTRACT. A set of models for estimating the enthalpy of formation, the entropy, the heat capacity and the volume of dehydrated phyllosilicates is presented. The model for entropy and heat capacity estimation is essentially based on a method of decomposition into polyhedral units, similar to that published by Holland (1989). The model for predicting the enthalpy of formation is based on the electronegativity scale, as previously developed by Vieillard (1994a, 1994b). For the sake of consistency, the models are parameterized using the same critical selection of thermodynamic properties from the literature. This includes a set of direct measurements especially dedicated to clay minerals that had not been taken into account in previous calculation methods. The accuracy of the predictions is tested for each property. The verification tests are also carried out for minerals that include different chemical elements than the phases used to derive the model constants, especially lithium-bearing micas. Verification tests also concern the Gibbs energy function that combines contributions from both models. Finally, the models are used in order to propose a complete thermodynamic database for clay mineral end-members. The consistency of the stability domains calculated on the basis of these thermodynamic properties is investigated by drawing relevant predominance diagrams for some chemical systems of interest. The models proposed represent a significant improvement with respect to previous works as regards the global accuracy of the estimates and because the developments were realized and tested using the same set of minerals, whose properties had been collected through a critical selection of the literature.

Keywords: clay mineral, thermodynamic data, enthalpy, Gibbs free energy, entropy, phyllosilicates, chlorite

INTRODUCTION

The long term stability of clay minerals is of critical importance, not only for academic reasons but also within the context of deep underground nuclear waste repositories, due to the sorption capacities and the plasticity of such materials. Numerous experiments have already demonstrated the ability of alkaline solutions stemming from cementitious materials (expected in deep repositories) to generate important transformations in clay rocks (Gaucher and Blanc, 2006). Such experiments usually concern time periods that are limited in relation to the timescales considered in safety assessment calculations. In order to extend the range of experiments, geochemical modeling has been used for a number of years as a valuable tool for predicting mineralogical and chemical evolutions (Gaucher and others, 2004; Marty and others, 2009). Thermodynamic properties are essential for such applications, but they are still poorly understood for clay minerals and, until very recently, little unambiguous experimental data were available. For example, numerous experimental studies of equilibration in solution have been conducted since the pioneering work of Reesman and Keller (1968). Equilibration experiments on illite were repeated by Kittrick (1984) and Aja and others (1991). The smectite case was investigated, among

* BRGM, 3 Avenue C. Guillemin, BP6009, F-45060 Orleans, France
** CNRS-IC2MP-UMR-7285 -Hydrasa, 5 Avenue Albert Turpain, 86022 POITIERS-Cedex, France
§ Andra, F-92298 Châtenay-Malabry Cedex, France.
†Corresponding author: p.blanc@brgm.fr

others, by Reesman and Keller (1968), May and others (1986) and Kittrick and Peryea (1988, 1989). Essene and Peacor (1995) strongly criticized the solution experiments and the properties derived from these studies have not as yet been included in the usual thermodynamic databases for geochemical modeling.

Moreover, an effort to acquire thermodynamic properties using calorimetric techniques has recently been made and full sets of parameters can be measured directly for illite, montmorillonite and beidellite (Gailhanou and others, 2012), saponite, vermiculite and nontronite (Gailhanou and others, 2013) and berthierine and chlorite (Blanc and others, 2013). This concerns essentially the minerals in their anhydrous states. The use of calorimetric devices avoids having to assess equilibrium achievement with respect to an aqueous solution, thereby providing reliable data for calculating equilibrium constants.

However, all of these measurements may not be sufficient for modeling studies involving clay minerals. Since clay minerals display variable composition, the probability is low that measured properties from the literature are directly usable. In addition, it is also of importance, for modeling studies, to consider the thermodynamic properties of a large variety of clay end-members that could possibly form from the primary phases, given the considered physical-chemical perturbations involved.

Predictive models could be used for this purpose. Furthermore, it has already been demonstrated that available methods are not accurate for clay minerals (Gailhanou and others, 2012, 2013) and that the combination of different methods may be questionable from a consistency point of view (Blanc and others, 2013). In order to address this issue, we propose herein a consistent suite of models for the prediction of ΔG^0_f, ΔH^0_f, S^0, Cp(T) and V for anhydrous clay minerals, parameterized using calorimetric data from the literature. The basis of the models stems from already published methods (Chermak and Rimstidt, 1989; Vieillard, 1994a, 1994b). The latter are refined and extended in order to predict consistently the full set of ΔG^0_f, ΔH^0_f, S^0, Cp(T) and V parameters, using a single set of data for parameterization and verification. In addition, the developments have been performed so as to be able to predict the properties of minerals that could include some unusual elements (such as Zn, Ni, Li, *et cetera*). More precisely, two types of predictive models have been developed:

— One is based on site specific interactions and uses an electronegativity scaling of the excess energies. It applies specifically to the prediction of ΔH^0_f (Vieillard, 1994a, 1994b).

— The other one relies on a conventional polyhedral decomposition method and is well suited for predicting properties that involve less specific interactions such as S^0, Cp(T) and V.

A critical selection of thermodynamic properties is performed from the literature, including parameters only from phyllosilicates. The models are parameterized using this dataset, ensuring compatibility and improving the accuracy of the predictions for phyllosilicates. Also, since the parameterization uses the same dataset, consistency is ensured between the two types of models. The models are verified by:

— Comparing the results with thermodynamic parameters *not lying within the* parameterization set.

— Creating predominance diagrams in order to check phase relations of end-members with respect to other minerals.

— Predicting properties for minerals including elements out of the parameterization set and comparing them with direct measurements.

This last point makes it possible to check the robustness of the model and its sensitivity to unusual compositions.

PRELIMINARY CONSIDERATIONS

This section presents the general conventions used in the present work, a review of the available predictive methods for the thermodynamic properties of solids and a critical selection of thermodynamic properties for clay minerals and phyllosilicates.

Thermodynamic Conventions and Relations

Classical thermodynamic relations and conventions theoretically apply to clay minerals as to any other mineral. Consequently, the formation properties of a clay mineral will depend on the definition of a reference state. The reference state is considered as the standard state, at 0.1 MPa and 298.15K. Following Helgeson and others (1978), the pressure between the temperature interval 273.15 to 373.15K is constant, at 0.1 MPa. For T > 373.15K (100 °C), the pressure is obtained from the water liquid-vapor curve. Considering a phase AB, its apparent Gibbs free energy of formation $\Delta G^0_{a,P,T}(AB)$ is given, at P and T, by the relation:

$$\Delta G^0_{a,P,T}(AB) = \Delta H^0_{a,P,T}(AB) - T\cdot\Delta S^0_{a,P,T}(AB) = \Delta H^0_{f,Pr,Tr}(AB) - T\cdot\Delta S^0_{f,Pr,Tr}(AB)$$

$$+\int_{Tr}^{T} C_p(AB)\,dT - T\cdot\int_{Tr}^{T}\frac{C_p(AB)}{T}dT + \int_{Pr}^{P} V(AB)\,dP = \Delta G^0_{f,Pr,Tr}(AB) - T\cdot S^0_{Pr,Tr}(AB)$$

$$+\int_{Tr}^{T} C_p(AB)\,dT - T\cdot\int_{Tr}^{T}\frac{C_p(AB)}{T}dT + \int_{Pr}^{P} V(AB)\,dP \quad (1)$$

with:

— T_r the temperature at the reference state (= 298.15K)

— P_r the pressure at the reference state (= 0.1 MPa)

— $\Delta H^0_{f,Pr,Tr}(AB)$ the enthalpy of formation of phase AB at the temperature and pressure of reference T_r and P_r

— $S^0_{Pr,Tr}(AB)$ the third law entropy of phase AB

— Cp(AB) the heat capacity of phase AB

— V(AB) the molar volume of phase AB, independent of temperature.

This definition follows the Benson–Helgeson convention (Helgeson and others, 1978) where, basically, the heat capacities of the elements are not considered. In this case, $\Delta G^0_{a,P,T}(AB)$ equals $\Delta G^0_{f,P,T}(AB)$ only at 25 °C. Concerning the Cp(T) function, its temperature dependence is expressed in the present work by the Maier-Kelley polynomial expression where $Cp(T) = a + bT - c/T^2$. The third law entropy term, at T_r, includes the heat capacity function, and a residual contribution:

$$S^0_{Pr,Tr}(AB) = \int_0^{Tr}\frac{C_p(AB)}{T}\,dT + S^{mag}(AB) + S^{conf}(AB) \quad (2)$$

The two first terms in equation (2) can be measured by low temperature calorimetry [PPMS or adiabatic, see Gailhanou and others, (2012) for details] and S^{mag} represents the magnetic entropy. As explained by Holland (1989), only the first term in equation (2), that is to say $S^{lat}=S^0_{Pr,Tr}-S^{conf}-S^{mag}$, where S^{lat} corresponds to the crystalline lattice entropy. For clay minerals, recent studies (Gailhanou and others, 2007, 2012; Gailhanou and Blanc, 2009; Blanc and others, 2013) have demonstrated that the magnetic

contribution is difficult to detect and to measure directly. Instead, Ulbrich and Waldbaum (1976) have proposed a calculation method for assessing the maximum value of both the magnetic and the configurational entropy terms. For the S^{conf} term, the method is based on a site mixing approach and, for the magnetic contribution, on the maximum number of spin configurations according to:

$$S^{mag} = R \sum_{i} x_i \ln(2S_i + 1) \tag{3}$$

where R is the gas constant, x_i the amount of element i and S_i its spin number. This expression is valid for the metals of the first transition series where the valence electrons are in the outermost shells.

Considering again the AB solid, we can express its equilibrium in aqueous media with the dissolved species A^+ and B^-:

$$A^+ + B^- \xleftrightarrow{\Delta\Xi^0_{r,P,T}(AB)} AB \tag{4}$$

Any reaction property $\Delta\Xi^0_{r,P,T}(AB)$ can be obtained from the corresponding formation property $\Delta\Xi^0_{f,P,T}(AB)$, according to the relation:

$$\Delta\Xi^0_{r,P,T}(AB) = \Delta\Xi^0_{f,P,T}(AB) - \Delta\Xi^0_{f,P,T}(A^+) - \Delta\Xi^0_{f,P,T}(B^-) \tag{5}$$

where Ξ stands for G, H, S, or any other property. Finally, the Gibbs free energy of reaction (4) is related to the equilibrium constant of the reaction, $K_{P,T}(AB)$, by:

$$\Delta G^0_{r,P,T}(AB) = -R \cdot T \cdot \mathrm{Log}K_{P,T}(AB) \cdot \ln(10) \tag{6}$$

In the case of reaction (4), according to the Mass Action Law, the equilibrium is reached when:

$$\mathrm{Log}K_{P,T}(AB) = \frac{[AB]}{[A^+] \cdot [B^-]} \tag{7}$$

where bracketed symbols correspond to activities. The thermodynamic properties of the aqueous complexes used in this work are issued from the Thermochimie database (Giffaut and others, 2014).

Estimation Methods

To determine the missing thermodynamic parameters of a clay mineral phase whose chemical composition is known, different methods have been developed using thermodynamic data of other silicates in order to estimate the major thermodynamic parameters (V, ΔG^0_f, ΔH^0_f, S^0, Cp_{Tr}). This section provides a brief overview of the five different classes of methods developed to date and available in the literature.

Comparative methods.—Comparative methods use the thermodynamic similarities of compounds sharing the same anions or cations. They are based on simple relationships between selected clay mineral compounds. Sverjensky (1985) and Sverjensky and Molling (1992) established a set of linear relationships between the free standard enthalpies of formation of clay minerals and of divalent ions in aqueous species.

Statistical methods.—Statistical methods can describe the thermodynamic functions either as a linear combination of a variable such as the mineral stoichiometric composition, or as a function of several chemical and physical variables. Using only stoichiometry, a clay mineral can be decomposed into a sum of oxides and/or hydroxides of all cations, in such a way that the properties (ΔG^0_r, ΔH^0_r, ΔS^0_r, ΔV_r,

ΔCp_r) of fictive solid-solid reactions are zero. This method is the most widely used for predicting the value of different thermodynamic entities, that is the enthalpy of formation of micas, smectites and chlorites (Chermak and Rimstidt, 1989; Van Hinsberg and others, 2005a), the free energies of formation of micas (Chermak and Rimstidt, 1989) and smectites (Tardy and Garrels, 1974; Nriagu, 1975); the entropy and molar volumes of clay minerals (Helgeson and others, 1978; Holland, 1989; Van Hinsberg and others, 2005b) and the heat capacity of clay minerals (Helgeson and others, 1978; Robinson and Haas, 1983; Berman and Brown, 1985).

Another statistical method developed by Kashik and others (1978) enables the Gibbs free energy of formation of any phyllosilicate to be determined by a combination of stoichiometric components and molar volumes through multivariable regression.

Parametric methods.—In these methods, the parameters used in the prediction of thermodynamic entities can be empirical (electronegativity) or characteristics of other clay mineral properties. The concept of the electronegativity χ was defined by Pauling (1960) as the power of an atom in a molecule to attract electrons from another atom. The greater the difference in electronegativity between atoms and oxygen, the higher the energy of formation of the compound. Considering a binary oxide ABO_N (where A and B are different cations), it may be decomposed into a sum of two oxides AO_{n1} and BO_{n2}. The energy of formation of ABO_N can be written as:

$$E(ABO_N) = E(AO_{n1}) + E(BO_{n2}) + kX_AX_B(\chi_A - \chi_B)^2 \quad (8)$$

The last term, representing the energy of formation of the compound from AO_{n1} and BO_{n2}, is proportional to the molar fraction of oxygen atoms related to the cations A (X_A) and B (X_B) and to the electronegativity difference between the cations A and B bonded to the same oxygen atom. Zuyev (1987) predicted the enthalpy of formation based on the electronegativity of a constant and single ion, while Vieillard (1994a, 1994b) derived the enthalpy of formation from experimental data of several compounds (silicates, aluminates and ferrites). In the latter case, the author considered the electronegativity of an ion as being a function of the interatomic distance between the ion and the oxygen, involving the so-called Born-Haber energy. For both hydrated and dehydrated clay minerals, Vieillard (2000, 2002) estimated the Gibbs free energy from the electronegativity difference concept.

Similar to this approach, Mattigod and Sposito (1978) have proposed considering the Gibbs free energies of formation from oxides and hydroxides as a function of a parameter that depends on the nature of the isomorphic substitutions, ionic radii and charge of interlayer cations. This method has been refined by Sposito (1986) by introducing a specific correction term.

Solid solution models.—The use of solid solution models in interpreting the composition and stability of clay mineral phases was promoted by the work of Weaver and Pollard (1973) and Velde (1977). The different solid solution models can be classified into two categories, ideal mixing models and non-ideal, regular mixing models.

In the first category, different models may exist and can be distinguished by the nature of the crystallographic sites considered. The simplest model is based on a random mixing of cations in energetically equivalent sites. This is the case of models developed by Helgeson and Mackenzie (1970), Aagaard and Helgeson (1983), and Helgeson and Aagaard (1985) for smectites. Tardy and Fritz (1981) developed a model with 36 end-members, based on molar ideal mixing, independently of the chemical composition. Tardy and Duplay (1992) developed a model for hydrated and anhydrous smectites from the model initiated by Tardy and Fritz (1981). For chlorites, a first model based on a set of six end-members was proposed by Walshe (1986), followed by Bryndzia and Scott (1987), McPhail and others (1990), Aagaard and Jahren (1992) and Saccocia and Seyfried (1994). Holland and others (1998) and Holland and Powell

(1998) finally proposed their own three site mixing model for micas and a four site mixing model for chlorites.

The second group was initially proposed by Stoessell (1979) with four micaceous end-members and a three site regular mixing model. It was improved by considering a canonical function of cation distribution (Stoessell, 1981) and was extended to four sites for chlorites (Stoessell, 1984). Since then, different models based on three or four site regular mixing have been developed for illites, micas and chlorites (Vidal and others, 2001; Coggon and Holland, 2002; Parra and others, 2002, 2005). Considering asymmetrical subregular mixing, Massonne and Szpurka (1997) built a model for (Mg, Fe) celadonite. In this case, two Margules parameters are necessary to explain the behavior of a binary solid solution as shown by Eugster and others (1972), Chatterjee and Flux (1986) and Roux and Hovis (1996) for the muscovite-paragonite joint.

Other models.—By considering the free enthalpy of formation $\Delta G^0_r = \Delta G^0_f$ (mineral) $-\Sigma\Delta G^\circ_{f,i}$ in which $\Sigma\Delta G^\circ_{f,i}$ represents the sum of the free standard enthalpies of formation of reaction compounds, Chen (1975) assumed an exponential variation of ΔG^0_r with the nature and the complexity of reaction compounds. This model was refined by Varadachari and others (1994) and applied to clay minerals.

Assessment of some predictive methods for clay minerals.—Gailhanou and others (2012, 2013) have attempted to assess some estimation methods among the most popular with respect to thermodynamic properties measured directly by calorimetric means, for the minerals illite, montmorillonite, beidellite, nontronite, saponite and vermiculite. They concluded that:

— To estimate the full set of thermodynamic properties for a clay mineral, a combination of several methods is required, which poses the problem of the consistency of the estimates.

— Discrepancies in calculating ΔG^0_f, ΔH^0_f and S^0 concern both the accuracy and the precision, that is both a scattering of predictions with respect to the experimental values and a systematic deviation.

— The latter case is well illustrated by comparing the entropy values predicted using the Holland (1989) model with experimental measurements. Gailhanou and others (2013) have pointed out a systematic deviation of -36 J/mol.K for the calculations, which corresponds to more than 10 percent of the measured value.

— For heat capacity, the systematic error with the Berman and Brown (1985) model is less important, reaching -10 J/mol.K (Gailhanou and others, 2013).

— Predictions made for ΔH^0_f using the Chermak and Rimstidt (1989) method also display a systematic -20 kJ/mol deviation for illite, montmorillonite, beidellite and saponite. For nontronite and vermiculite, the deviation dramatically increases up to -150 kJ/mol, also producing a general scattering of 130 kJ/mol of the calculation results with respect to the measurements.

In conclusion, given the aforementioned performance, current estimation methods can hardly be used to predict the thermodynamic properties of clay mineral end-members and include them in a general thermodynamic database for geochemical calculations. The present work aims to fill this gap.

Selection of the Thermodynamic Constants for Model Development

This section is dedicated to a selection of thermodynamic properties for phyllosilicates derived from the literature. This selection is to be used:

— to parameterize the models,
— to verify the models,
— directly, to implement the clay minerals database.

The selection of thermodynamic constants is an essential step in developing prediction models. Here the selection conforms to the following rules:

— to enhance direct and traceable measurements,
— to select data only for phyllosilicates,
— to discard estimated values, when possible.

These rules are established in order to focus the selection on phyllosilicates, which is also a way to increase, *a priori*, the accuracy of the method for clay minerals by including interaction contributions specific to structurally similar minerals into the constants derived for the models. It also seems important to enhance directly measured data, for the sake of accuracy and traceability and in order to remain consistent with the general thermodynamic relations. However, when no other data are available, properties derived from equilibrium experiments performed at high temperature and pressure are also selected. A recent and different work was performed by Tutolo and others (2014) who focused on a set of 12 minerals and 10 aqueous complexes in the chemical system Na_2O-K_2O-SiO_2-Al_2O_3-Cl-CO_2-H_2O. The authors managed to refine the thermodynamic properties of the different phases in the system, consistently, using the results from high temperature and pressure equilibrium experiments. The present work is taking place in a different framework, that is the development of a large thermodynamic database (Giffaut and others, 2014; Grivé and others, 2015; Blanc and others, 2015), especially devoted to the modeling of cement/clay interactions (among other applications). The clay minerals compositions we are considering are ranging in an 8 dimension space (Si, Al, Mg, FeII, FeIII, K, Na, Ca) at least. The full database itself now includes more than 60 elements, not to mention the organics. A full refinement is not feasible in that case. Instead, the choice was made to rely on the critical selection of thermodynamic properties, with selection guidelines explained previously and detailed by Giffaut and others (2014) and Blanc and others (2015). Refined properties are avoided, as far as possible.

For most of the minerals retained for calibration, we have selected a complete set of thermodynamic data [ΔH^0_f, S^0, V, and Maier-Kelley coefficients a, b and c for the Cp(T) function]. All the selected phases are given in tables 1 and 2 and a more detailed discussion is provided in Appendix 1.

Verification of phase relations is performed by assessing predominance diagrams in sub-systems of interest with respect to observations from experiments or field studies. As reported by Gailhanou and others (2012, 2013) and Blanc and others (2013, 2014), results from high temperature and high pressure experiments can hardly be used without making various hypotheses that strongly lessen the meaning of the demonstration.

General Context for Predictive Model Developments

This section provides explanations about the types of models developed in the present work, their connections, the verification tests and their "extrapolation" capacities.

Consistency issues.—The need for unifying predictive approaches arises clearly with some recent tests against consistent sets of thermodynamic parameters acquired recently by calorimetric means (Gailhanou and others, 2012, 2013). The tests favored the use of Chermak and Rimstidt (1989), Holland (1989) and Berman and Brown (1985) methods for predicting respectively ΔG^0_f, S^0 and Cp(T) of clay minerals. Apart from the precision and accuracy problems revealed by the tests, it was also shown that, for the Chermak and Rimstidt (1989) method, ΔH^0_f displayed a greater discrepancy with respect to experimental data than ΔG^0_f, indicating an internal consistency problem. The problem could have been partially solved by combining the Chermak

TABLE 1

Thermodynamic properties of phyllosilicates, used for parameterizing the models

d001	Mineral	Formula	ΔH^0_f kJ.mol^{-1}	Ref.	S^{conf} J.mol^{-1}. K^{-1}	S^{mag} J.mol^{-1}. K^{-1}	S^0 J.mol^{-1}.K^{-1}	Ref.	V cm^3.mol^{-1}	Ref.	Cp (25°C) J.mol^{-1}. K^{-1}	a J.mol^{-1}. K^{-1}	b*10^3 J.mol^{-1}. K^{-2}	c*10^{-5} J.mol^{-1}. K	Ref.
10 Å	Muscovite	$KAl_2(Si_3Al)O10(OH)_2$	-5974.80 ± 4.9(0.08)	(1)	18.70		306.40 ± 0.6(0.20)	(16)	140.81	(2)	325.99	335.80	232.25	-70.27	(16)
	Pyrophyllite	$Al_2Si_4O_{10}(OH)_2$	-5640.00 ± 1.5(0.03)	(2)			239.40 ± 0.4(0.17)	(16)	128.10	(2)	293.76	314.07	198.15	-70.57	(16)
	Phlogopite	$KMg_3(Si_3Al)O10(OH)_2$	-6215.00 ± 3.5(0.06)	(4)	18.70		334.60 ± 1.0(0.30)	(18)	149.65	(2)	354.65	382.60	192.44	-75.85	(18)
	Annite	$KFe_3(Si_3Al)O10(OH)_2$	-5130.97 ± 8.3(0.16)	(5)		40.14	424.02 ± 8.4(1.98)	(5)	154.30	(2)	390.32	424.70	200.16	-83.62	(2)
	Talc	$Mg_3Si_4O_{10}(OH)_2$	-5892.10 ± 4.0(0.07)	(6)			260.80 ± 0.6(0.23)	(19)	136.20	(2)	321.77	420.73	89.19	-111.61	(21)
	Smectite MX80	(b)	-5656.37 ± 5.4(0.10)	(14)	24.41	4.18	301.92 ± 0.2(0.07)	(14)	134.92	(14)	322.74	318.58	281.53	-70.92	(14)
	Illite IMt-2	(c)	-5711.25 ± 8.5(0.15)	(14)	29.86	6.97	324.92 ± 0.2(0.06)	(14)	139.18	(14)	328.21	371.32	182.59	-86.72	(14)
	Vermiculite SO	(e)	-6034.41 ± 5.7(0.09)	(15)	26.66	4.80	325.77 ± 0.5(0.15)	(15)	148.36	(15)	346.39	329.42	313.40	-67.98	(15)
	Nontronite Nau-1	(d)	-5035.69 ± 5.3(0.11)	(15)	24.87	33.49	332.75 ± 7.0(2.10)	(15)	136.38	(15)	335.15	289.85	363.09	-55.96	(15)
	Paragonite	$NaAl_2(Si_3Al)O10(OH)_2$	-5937.50 ± 3.0(0.05)	(7)			277.10 ± 0.9(0.32)	(18)	132.10	(2)	321.50	337.88	220.78	-73.08	(18)
	Margarite	$CaAl_2(Si_2Al_2)O10(OH)_2$	-6244.00 ± 2.6(0.04)	(2)			263.60 ± 0.3(0.11)	(2)	129.63	(2)	323.41	347.58	216.85	-78.96	(2)
	Minnesotaite	$Fe_3Si_4O_{10}(OH)_2$	-4822.99	(9)		40.14	350.80	(9)	148.50	(9)	364.40	411.38	125.52	-75.03	(9)
	Mg-Celadonite	$KMgAlSi_4O_{10}(OH)_2$	-5834.74	(22)	11.53		291.00	(22)	139.62	(22)	325.75	357.09	205.51	-82.32	(10)
	Fe-Celadonite	$KFeAlSi_4O_{10}(OH)_2$	-5478.13	(22)	11.53	13.38	330.17	(22)	143.01	(22)	331.48	354.09	215.67	-77.26	(10)
	Eastonite	$K(Mg_2Al)(Si_2Al_2)O_{10}(OH)_2$	-6348.94 ± 4.7(0.07)	(10)	10.60		306.00	(10)	147.51	(10)	350.96	385.32	195.60	-82.39	(10)
	Siderophyllite	$K(Fe_2Al)(Si_2Al_2)O_{10}(OH)_2$	-5628.27 ± 4.2(0.07)	(11)	10.60	26.76	375.00	(11)	150.63	(11)	363.18	379.43	218.12	-72.26	(11)
14 Å	Amesite	$Mg_4Al_2(Al_2Si_2)O_{10}(OH)_8$	-9035.90	(12)			403.20	(12)	205.20	(12)	540.47	600.70	340.86	-143.88	(12)
	Fe-Amesite	$Fe_4Al_2(Al_2Si_2)O_{10}(OH)_8$	-7607.46	(12)		53.53	514.80	(12)	209.00	(12)	564.74	595.11	375.34	-126.88	(12)
	Clinochlore	$Mg_5Al(AlSi_3)O_{10}(OH)_8$	-8909.59	(12)			435.15	(12)	211.47	(12)	516.34	631.95	282.68	-177.69	(12)
	Chamosite	$Fe_5Al(AlSi_3)O_{10}(OH)_8$	-7120.85	(12)		66.91	559.40	(12)	215.88	(12)	574.76	599.55	372.80	-120.85	(12)
	Sudoite	$Mg_2Al_4Si_3O_{10}(OH)_8$	-8655.27	(12)			390.50	(12)	205.10	(12)	509.72	557.84	351.23	-135.86	(12)
	Ripidolite Cca-2	(a)	-8240.14 ± 8.6(0.10)	(23)		27.60	469.40 ± 2.9(0.62)	(20)	211.93	(13)	547.02	587.00	392.11	-139.46	(20)
7 Å	Kaolinite	$Al_2Si_2O_5(OH)4$	-4115.30 ± 4.1(0.10)	(3)			200.90 ± 0.5(0.25)	(17)	99.34	(2)	243.37	282.05	123.62	-67.15	(17)
	Lizardite	$Mg_3Si_2O_5(OH)_4$	-4362.00 ± 3.0(0.07)	(8;2)			216.30 ± 0.8(0.37)	(8;2)	107.50	(2)	274.14	296.63	167.14	-64.29	(2)
	Antigorite	$Mg_{48}Si_{34}O_{85}(OH)_{62}$	-71417.98 ± 19.9(0.03)	(10)			3591.00	(10)	1754.80	(10)	4380.66	4952.60	2422.78	-1150.54	(10)

Uncertainties given in absolute values and between parentheses in percentage Formulas: (a) $(Mg_{2.96}Fe^{2+}_{1.71}Fe^{3+}_{0.22}Al_{1.12}Ca_{0.01})(Si_{2.63}Al_{1.37})O_{10}(OH)_8$; (b) $(Na_{0.409}K_{0.024}Ca_{0.009})(Si_{3.738}Al_{0.262})(Al_{1.598}Mg_{0.214}Fe^{3+}_{0.173}Fe^{2+}_{0.035})O_{10}(OH)_2$; (c) $K_{0.762}Na_{0.044}(Si_{3.387}Al_{0.613})(Al_{1.427}Fe^{3+}_{0.292}Mg_{0.241}Fe^{2+}_{0.084})O_{10}(OH)_2$; (d) $Ca_{0.247}K_{0.020}(Si_{3.458}Al_{0.542})(Fe^{3+}_{1.688}Al_{0.276}Mg_{0.068})O_{10}(OH)_2$; (e) $Ca_{0.445}(Si_{2.778}Al_{1.222})(Al_{0.192}Mg_{2.468}Fe^{3+}_{0.226}Fe^{2+}_{0.028}Ti_{0.018}Mn_{0.007})O_{10}(OH)_2$

(1) - Haselton and others (1995); (2) - Robie and Hemingway (1995); (3) - Fialips and others (2001); (4) - Circone and Navrotsky (1992); (5) - Dachs and Benisek (1997); (6) - Kahl and Maresch (2001); (7) - Roux and Hovis (1996); (8) - Evans (2004); (9) - Miyano and Klein (1983); (10) - Holland and Powell (1998); (11) - Holland and Powell (1990); (12) - Vidal and others (2005); (13) - Gailhanou and others (2009); (14) - Gailhanou and others (2012); (15) - Gailhanou and others (2013); (16) - Robie and others (1976); (17) - Robie and Hemingway (1991); (18) - Robie and Hemingway (1984); (19) - Robie and Stout (1963); (20) - Gailhanou and others (2007); (21) - Krupka and others (1979); (22) - Parra and others (2002); (23) - Blanc and others (2014)

TABLE 2

Thermodynamic properties of phyllosilicates, used for verifying the models

	Mineral	Formula	ΔH^0_f kJ.mol^{-1}	Ref.	S^{conf} J.mol^{-1}.K^{-1}	S^{mag} J.mol^{-1}.K^{-1}	S^0 J.mol^{-1}.K^{-1}	Ref.	V cm^3.mol^{-1}	Ref	Cp (25°C) J.mol^{-1}.K^{-1}	a J.mol^{-1}.K^{-1}	b*10^3 J.mol^{-1}.K^{-2}	c*10^{-5} J.mol^{-1}.K	Ref.
10 Å	Illite	(a)					276.05 ± 0.6(0.22)	(7)	144.25	(10)	322.75				(7)
	Na-Phlogopite	$NaMg_3AlSi_3O_{10}(OH)_2$	-6172.14 ± 2.2(0.04)	(1)			318.00	(1)	144.50	(1)	355.11	395.44	180.49	-83.69	(1)
	Saponite SapCa-2	(b)	-5994.06 ± 4.9(0.08)	(4)	17.83	0.28	314.55 ± 1.6(0.51)	(4)	141.66	(4)	346.97	347.26	274.68	-73.06	(4)
	Beidellite SBId-1	(c)	-5720.69 ± 6.5(0.11)	(5)	21.43	2.23	293.52 ± 0.4(0.14)	(5)	137.98	(5)	318.58	253.39	373.04	-40.92	(5)
	Vermiculite	(d)	-5859.00	(13)											
	Siderophyllite	$K(Fe_2Al)(Si_2Al_2)O_{10}(OH)_2$	-5622.00 ± 15.0(0.27)	(6)											
14 Å	Fe-Sudoite	$Fe_2Al_4Si_3O_{10}(OH)_8$	-7912.77 ± 2.3(0.03)	(1)		26.76	457.00	(1)	204.00	(1)	605.61	631.07	440.26	-139.32	(1)
	Mg-chlorite	$Mg_6Si_4O_{10}(OH)_8$	-8744.20 ± 2.3(0.03)	(1)			408.00	(1)	216.60	(1)	521.31	605.06	327.39	-161.22	(1)
	High-Mg chlorite	(e)				12.69	431.70 ± 5.0(1.16)	(8)			535.60	561.80	398.79	-128.98	(8)
	High-Fe chlorite	(f)				44.03	495.70 ± 10.0(2.02)	(8)			540.20	547.97	386.80	-109.42	(8)
	Clinochlore	$Si_3Al(Mg_5Al)(O_{10}(OH)_8)$			11.50		437.10 ± 0.4(0.09)	(2)			529.40	582.57	329.28	-134.54	(2)
	Chamosite	$(Si_3Al)(Fe_5Al)O_{10}(OH)_8$			11.50	66.91	583.50 ± 0.2(0.03)	(2)			572.40	610.55	344.98	-125.34	(2)
7 Å	Berthierine	$(Fe^{2+}_{2.5}Al_{0.5})(Si_{1.5}Al_{0.5})O_5(OH)$				23.37	284.10 ± 0.3(0.11)	(9)	107.10	(9)	270.87	314.19	76.25	-58.72	(9)
	Greenalite	$Fe_3Si_2O_5(OH)_4$	-3301.00	(3)		40.14	304.50	(3)	115.00	(3)	302.32	303.39	166.34	-45.04	(3)

Uncertainties given in absolute values and between parentheses in percentage Formulas: (a) $(K_{0.75})(Si_{3.50}Al_{0.50})(Al_{1.75}Mg_{0.25})O_{10}(OH)_2$; (b) $(Na_{0.394}K_{0.021}Ca_{0.038})(Si_{3.569}Al_{0.397})(Mg_{2.949}Fe_{0.034}{}^{3+}Fe_{0.021}{}^{2+})O_{10}(OH)_2$; (c) $Ca_{0.185}K_{0.104}(Si_{3.574}Al_{0.426})(Al_{1.812}Mg_{0.090}Fe^{+3}{}_{0.112})O_{10}(OH)_2$; (d) $(Ca_{0.1}Mg_{0.4})(Mg_{2.7}Fe^{2+}{}_{0.1}Fe^{3+}{}_{0.2})(Si_3Al_{0.8}Fe^{3+}{}_{0.2})O_{10}(OH)_2$; (e) $(Si_{2.99}Al_{1.01})(Al_{1.39}Fe^{3+}{}_{0.21}Fe^{2+}{}_{0.57}Mg_{3.52})O_{10}(OH)_8$; (f) $(Si_{2.47}Al_{1.53})(Al_{1.60}Fe^{2+}{}_{3.29}Mg_{1.05})O_{10}(OH)_8$

(1) - Holland and Powell (1998); (2) - Bertoldi and others (2007); (3) - Miyano and Klein (1983); (4) - Gailhanou and others (2013); (5) - Gailhanou and others (2012); (6) – Ogorodova and others (2009); (7) - Robie and others (1976); (8) – Hemingway and others (1984); (9) - Bertoldi and others (2005); (10) - Robie and Hemingway (1995)

and Rimstidt (1989) and Holland (1989) methods for calculating ΔH^0_f. However, in addition to the internal inconsistencies induced by the process, the consequences for estimating a thermodynamic property using two different methods with two different parameterizing data sets are difficult to predict.

Instead, some authors have tried to develop generalized methods that could apply to any property, ensuring internal consistency of the predicted values. Among these, La Iglesia and Félix (1994) have proposed a method that applies specifically to carbonates. Van Hinsberg and others (2005a, 2005b) have published the only generalized method that could apply to phyllosilicates. In the latter, the properties are refined after the Holland and Powell (1998) database, which has itself been refined from experiments performed mainly at T> 300 °C. The application domain is therefore mainly devoted to rather high temperature domains and Gailhanou and others (2012) have already found large discrepancies between properties calculated with the Van Hinsberg and others (2005a) method and the values directly measured for illite, montmorillonite and beidellite.

Developing a generalized model for anhydrous clay minerals.—In developing a generalized model, a first point is to verify the quality of the estimates. It was then important to estimate properties that could be measured directly, for comparison purposes. It was thus preferred to propose a method for predicting ΔH^0_f rather than ΔG^0_f. For this reason, since the available statistical methods failed to provide accurate estimates of experimental values (Gailhanou and others, 2012), we selected a different type of previously developed model and tried to improve its results for clay minerals. We selected the parametric method previously proposed by Vieillard (1994a, 1994b), which includes anion-cation interactions that can be refined specifically for a group of given minerals. In addition, it has the capacity to extend its predictions to chemical elements that do not belong to the parameterizing set (allowing estimates for Li-, Zn- or Cd-bearing clay minerals for example).

For the other properties, either the statistical method seemed to provide good results [such as the Berman and Brown (1985) method for estimating Cp] or a systematic deviation was observed (Gailhanou and others, 2013). In that case, focusing more the refinement process on clay minerals could significantly improve the accuracy of the methods. A statistical method similar to that of Holland (1989) or Chermak and Rimstidt (1989) was retained for the estimates of S^0 and each of the a, b and c Maier-Kelley coefficients for Cp(T) and V.

The consistency between both models is ensured in different ways:

— by using the same set of minerals to derive the respective model constants,
— by using the same set of minerals to verify the accuracy of the estimates for each property,
— by combining both ΔH^0_f and S^0 and verifying the estimate of ΔG^0_f with respect to experimental values,
— by comparing the stability diagrams that can be drawn from estimated ΔG^0_f with field or laboratory observations.

Model for predicting the enthalpy of formation of clay minerals

Fundamental Developments

Crystallographic considerations.—The enthalpy prediction model developed here is based on a balance of anion-cation interactions within a crystal structure. Therefore, a brief description of the structure involved is given.

In the present work, three types of phyllosilicates are considered, depending on the layer type (tetrahedral, octahedral, interlayer and brucitic layers) and stacking (fig. 1).

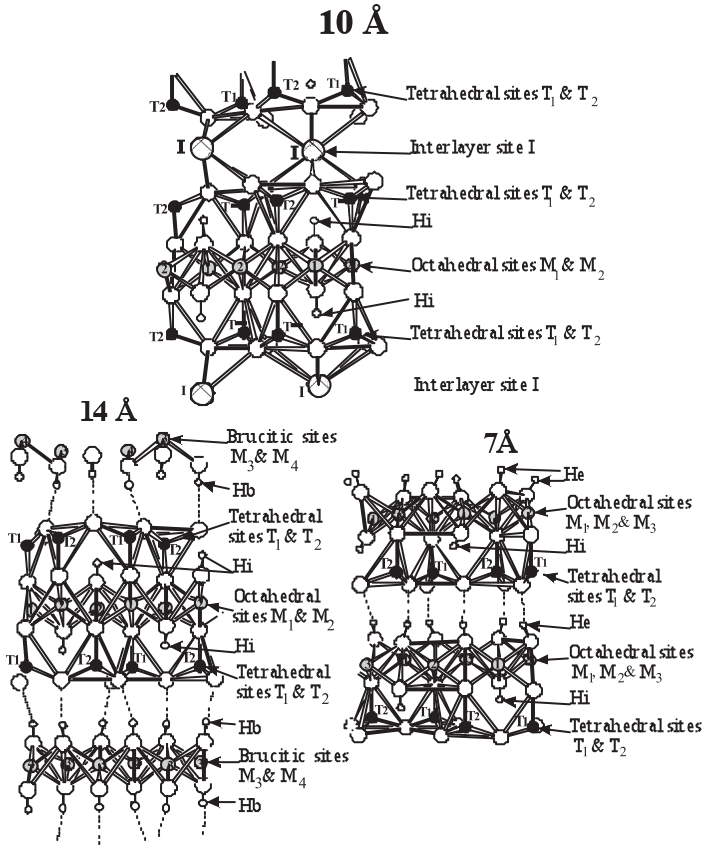

Fig. 1. Crystal structures of 10Å, 14Å and 7Å phyllosilicates showing the positions of the different crystallographic sites.

In a phyllosilicate, a layer can be composed either of: 1 tetrahedral + 1 octahedral sheet (1:1 layer), 2 tetrahedral + 1 octahedral sheet (2:1 layer) or the latter with a brucitic sheet in the interlayer (2:1:1 layer). These correspond respectively to the following structural formulas:

— 1:1 layer type (7 Å group, kaolinite, serpentines, *et cetera*):
$(M^{Zi^+}_{i,siteM_1})(M^{Zi^+}_{i,siteM_2})(M^{Zi^+}_{i,siteM_3})(M^{Zi^+}_{i,siteT_1})(M^{Zi^+}_{i,siteT_2})O_5(OH_i)(OH_e)_3$

— 2:1 layer type (10Å group, smectites, micas, *et cetera*):
$(M^{Zi^+}_{i,siteI})(M^{Zi^+}_{i,siteM_1})(M^{Zi^+}_{i,siteM_2})(M^{Zi^+}_{i,siteT_1})(M^{Zi^+}_{i,siteT_2})O_{10}(OH_i)_2$ where I is the interlayer site which is equal either to 0 (pyrophyllite, talc) or to 1 (micas, if M = K^+ or Na^+, brittle micas, if M= Ca^{2+} , or Ba^{2+}).

— 2:1:1 layer type (14Å group, chlorites):
$(M^{Zi^+}_{i,siteM_1})(M^{Zi^+}_{i,siteM_2})(M^{Zi^+}_{i,siteT_1})(M^{Zi^+}_{i,siteT_2})O_{10}(OH_i)_2(M^{Zi^+}_{i,siteM_3})(M^{Zi^+}_{i,siteM_4})(OH_b)_6$.

In dioctahedral micas and chlorites, the vacant octahedral site is located on the mirror plane of each 2:1 layer (generally M_1). In trioctahedral micas and chlorites, the arrangement of cations in site M_1 and in the two sites M_2 can depart from randomness (ordering). Such ordering can also be observed in the two sites M_3 and M_4 of the brucitic layers of chlorite minerals. Minerals belonging to the 7Å group exhibit three different sites M_1, M_2 and M_3. The labels i of H_i represent the proton located in the

TABLE 3

Enthalpies of formation of oxides and ions, at 298.15K, and parameter $\Delta_H O^{=} M^{z+}(aq)$ calculated for the selected cations

Oxides	ΔH^0_f (kJ.mol^{-1})	Ref.	Ions	ΔH^0_f (kJ.mol^{-1})	Ref.	$\Delta_H O^{=} M^{z+}(aq)$ (kJ.mol^{-1})
Na_2O	-414.80	(1)	$Na^+(aq)$	-240.34	(2)	65.80
K_2O	-363.17	(4)	$K^+(aq)$	-252.14	(2)	141.00
CaO	-634.92	(6)	$Ca^{+2}(aq)$	-543.00	(2)	-92.10
MgO	-601.60	(6)	$Mg^{+2}(aq)$	-467.00	(2)	-134.60
FeO	-272.04	(4)	$Fe^{+2}(aq)$	-90.00	(7)	-181.58
Fe_2O_3	-826.23	(8)	$Fe^{+3}(aq)$	-49.00	(7)	-242.43
Al_2O_3	-1675.70	(2)	$Al^{+3}(aq)$	-538.40	(9)	-199.63
SiO_2	-910.70	(10)	$Si^{4+}(aq)$	-	(5)	-205.0
H_2O ice II	-292.75	(3)	$H^+(aq)$	0.00	(11)	-292.75

(1) - Robie and Hemingway (1995); (2) - Cox and others (1989); (3) - Mercury and others (2001); (4) – Chase (1998); (5) - Vieillard and Tardy (1988a); (6) Garvin and others (1987), (7) – Parker and Khodakovskii (1995); (8) – Hemingway (1990); (9) Pokrovskii and Helgeson (1995); (10) Richet and others (1982); (11) By convention.

octahedral layer and oriented within the octahedral layer, for 1:1 and 2:1 phyllosilicates. The labels b and e of H_b and H_e represent the protons oriented towards the tetrahedral layers and located in the brucitic and the octahedral layer, for 2:1:1 and 1:1 phyllosilicates respectively.

Enthalpy prediction model development.—The enthalpy of formation of a mineral can be decomposed into sums that involve both the enthalpy of formation of the oxide of a given element and a specific term that accounts for the interactions of the element with the anions (oxygen atoms) in the given crystallographic site:

$$\Delta H^0_f(M_{k_1}M_{k_2}..M_{k_i}..M_{k_s}O_N) = \sum_{i=1}^{i=n_s} * (k_i * \frac{z_i}{2}) * \Delta H^0_f(M_i\ O_{xi})_{(c)} + \Delta H^0_{f,Ox} \qquad (9)$$

Each term of this general equation (9) is explained step by step in the following:

In equation (9), k_i and z_i are the stoichiometric coefficient and charge of a cation M in the oxide M_iO_{xi}. The enthalpies of formation of the oxides M_iO_{xi}, $\Delta H^0_f(M_iO_{xi})_{(c)}$, are shown in table 3 for each oxide of interest.

The enthalpy of formation of a compound from oxides $\Delta H^0_{f,Ox}$ is estimated by considering the specific interactions of the cations distributed among pairs of sites (Vieillard, 1994a):

$$\Delta H^0_{f,Ox} = -N[\sum_{k=1}^{k=n_S-1} \sum_{l=k+1}^{l=n_S} X_k X_l (\Delta_H O^{=}site{\cdot}k - \Delta_H O^{=}site{\cdot}l)] \qquad (10)$$

In equation (10), X_k and X_l are the molar fractions of the oxygen atoms related to the sites k and i, according to:

$$X_k = (1/N)(\sum_{i=1}^{i=n_{c,site.k}} n_{i,site.k} x_i) \qquad (11)$$

$$X_l = (1/N)\left(\sum_{i=1}^{i=n_{c,site.1}} n_{i,site.1} x_i\right) \quad (12)$$

In expressions (10), (11) and (12), n_s and n_c represent the number of sites and the number of cations, respectively. The total number of oxygen atoms bonded to the different cations, in all crystallographic sites of the phyllosilicate, must equal N:

$$\sum_{k=1}^{k=n_S i=n_{c,site.k}} \sum_{i=1} n_{i,site\cdot k} \cdot x_i = N \quad (13)$$

Each site may be occupied by one or more cations. For a given site, the parameter $\Delta_H O^=$(site) from equation (10) is the stoichiometric average of the parameters $\Delta_H O^=$(cation), expressed in terms of $\Delta_H O^= M_{i,clay}^{z_i+}$, increased by a term representing the energy of mixing between different cations:

$$\Delta_H O^=(site) = \frac{\sum_{i=1}^{i=n_S} x_i * (\Delta_H O^= M_i^{z_i+}(clay))}{\sum_{i=1}^{i=n_{sk}} n_i \cdot x_i.} + k_{mix} \cdot \sum_{i=1}^{i=nsj=nS-1} \sum_{j=i+1} (X_i) * (X_j)$$

$$* (\Delta_H O^= M_i^{z_i^+}(clay) - \Delta_H O^= M_j^{z_j^+}(clay)) \quad (14)$$

The mixing energy is valid only for interlayer, M_2 and M_3 sites because some different cations occupy the same site. For other sites such as M_1, M_4 and tetrahedral sites T_1 and T_2, the mixing site is not valid and $k_{mix}=0$. The parameters X_i and Xj_l are the molar fractions of the oxygen atoms related to the cations i and j in a specific site and are based on the total number of oxygen atoms bound to a given site.

In equation (14), the parameter $\Delta_H O^= M_{i,clay}^{z_i+}$, which characterizes the electronegativity of the cation i in the crystalline environment of the mineral, is calculated according to the following expression:

$$\Delta_H O^= M_{i,clay}^{z_i+} = 1/x_i \times [\Delta H_f^0 (M_i O_{x_i})_{(clay)} - \Delta H_f^0 (M_i^{z_i+})_{(c)}] \quad (15)$$

where $\Delta H_f^0 (MiO_{x_i})_{(clay)}$ and $\Delta H_f^0 (M_{iz_i}+)_{(c)}$ respectively indicate the enthalpy of formation of the oxide $M_i O_{x_i}$ and the ion $M_i^{z_i+}$ in the crystallized compound. The parameter $\Delta_H O^= M_{i,clay}^{z_i+}$ can be calculated from $\Delta_H O^= M_{i,ox}^{z_i+}$, which represents the oxygen affinity of the ion M^{z+} in pure oxide (Vieillard and Tardy, 1988a):

$$\Delta_H O^= M_{i,clay}^{z_i+} = \Delta_H O^= M_{i,ox}^{z_i+} + \delta\Delta_H O^= M^{z_i+} \quad (16)$$

In equation (16), the second term $\delta\Delta_H O^= M^{z_i+}$ is related to the modification of the site environment during the fictive transformation from the oxide $M_i O_{x_i}$ to the clay mineral.

The first term in equation (16), $\Delta_H O^= M_{i,ox}^{z_i+}$, corresponds to the electronegativity of a cation M^{zi+}in the stable oxide according to the expression (Vieillard and Tardy, 1988a, 1988b, 1989):

$$\Delta_H O^= M_{i,ox}^{z_i+} = 1/X_i \times [\Delta H_f^0 (M_i O_{x_i})_{(c)} - \Delta H_f^0 (M_i^{z_i+})_{(c)}] \quad (17)$$

This expression can also be applied to an aqueous cation, thus defining the parameter $\Delta HO^= M_{i,aq}^{z_i+}$ as:

$$\Delta_H O^{=} M^{z_i+}_{i,aq} = 1/X_i \times [\Delta H^0_f (M_i O_{x_i})_{(c)} - \Delta H^0_f (M_i^{z_i+})_{(aq)}] \quad (18)$$

where $\Delta H^0_f (M_i O_{x_i})_{(c)}$ and $\Delta H^0_f (M_i^{z_i+})_{(aq)}$ values are given in table 3. Additional explanations regarding equations (17) and (18) are proposed by Vieillard and Tardy (1988a).

Application to phyllosilicates.—Some simplifications are considered when applying the model to phyllosilicates, due to the structure of the minerals and also to the small number of data for the parameterization stage.

With respect to Vieillard's algorithm (1994a), the model assumes that the parameter $\Delta_H O^{=} M^{z+}{}_{(clay)}$, characterizing the electronegativity of the cation M^{Z+} in a specific site, is constant and independent on deviations in the interatomic variations of the various sites. For the tetrahedral sheet, two sites, T_1 and T_2, can be distinguished and the distribution of Si^{4+} and Al^{3+} among them obeys the rule of Loewenstein (1954), also detailed by Lipsicas and others (1984) and Sanz and Serratosa (1984). Specific interactions between sites (parameter k_{mix}) are taken into account only between the octahedral sites M_2 and M_3 and the interlayer site I in 10Å and 14Å phyllosilicates.

The present developments follow the principles of Pauling (1960) regarding the predominance of nearest-neighbor interactions (short-range interactions) observed in a crystal structure (Vieillard 1994a, 2000). The presence of a non-bridging oxygen atom between any two adjacent polyhedra in any phyllosilicate implies that long-range interaction energy terms between two sites are not required, and consequently:

$$\Delta_H O^{=} Site_i - \Delta_H O^{=} Site_1 = 0 \quad (19)$$

$$|\Delta_H O^{=} M^{z_i^+}_{i,site1} - \Delta_H O^{=} M^{z_j^+}_{j,site1}| = 0 \quad (20)$$

Contrary to the model developed by Vieillard (2000, 2002) on anhydrous smectites and phyllosilicates respectively, the model developed here is proposing a more realistic description of the cation distribution among the various sites. The second originality, related to the formalism developed by Vieillard (1994a, 1994b), is the use of energies of interactions between the cations occupying a same site.

Parameterizing the Model for Predicting the Enthalpy of Formation

The 24 selected minerals from table (3) are used to derive a set of sixteen parameters $\Delta_H O^{=} M^{z+}$ (clay) for the cations distributed in the various structural sites of the phyllosilicates:

— Na^+, K^+, Ca^{2+} in the interlayer sites (i),
— Mg^{2+}, Fe^{2+}, Fe^{3+}, Al^{3+} in the octahedral sites on the one hand (o) and in the brucitic sites on the other hand (b),
— Al^{3+} and Si^{4+} in the tetrahedral sites (t),
— H^+_o, H^+_b and H^+_e in the different sites.

In addition, the three mixing parameters among the three sites I, M_2 and M_3 are also refined. Finally, the global refinement process involves the determination of 19 unknown parameters. Constraints on minimization involve short-range interactions and positive value terms for the interaction energies between two different cations in accordance with equation (20).

The minimization is processed by fixing a new set of $\Delta_H O^{=} M^{z+}$ (clay) for sixteen ions in different sites (table 4). Then, assuming that $\Delta H^0{}_f(H^+)_{(c)} = 0$ J.mol^{-1} (Vieillard and Tardy, 1988a), the enthalpies of formation of H_2O in the three structural states are -254.10 kJ mol^{-1} within the octahedral layer (label o), -312.19 kJ mol^{-1} between the brucitic and the tetrahedral layers (label b) and –287.30 kJ mol^{-1} between the octahedral and tetrahedral layers (label e). Using the enthalpy of formation of ice II (Mercury and others, 2001), it appears that the protons in the brucitic layer (label b) oriented towards oxygen atoms of the tetrahedral layers are more strongly bonded to

TABLE 4

Values of the parameter $\Delta_H O^{=} M^{z+}$ (clay) for different ions and H^+ obtained by minimization

Cations [1]	Interlayer $\Delta_H O^{=} M^{z+}$(aq) (kJ mol^{-1})	$\Delta_H O^{=} M^{z+}$(i) (kJ mol^{-1})	Cations	Tetrahedral $\Delta_H O^{=} M^{z+}$(aq) (kJ mol^{-1})	$\Delta_H O^{=} M^{z+}$(t) (kJ mol^{-1})
K^+(i)	141.11	453.0	Si^4(t)	-205.00	-285.33
Na^+(i)	65.88	260.0	Al^{3+}(t)	-199.63	-260.45
Ca^{+2}(i)	-91.92	-71.22	Fe^{3+}(t)	-242.74	-310.00
	Octahedral			Brucitic	
	$\Delta_H O^{=} M^{z+}$(aq) (kJ mol^{-1})	$\Delta_H O^{=} M^{z+}$(o) (kJ mol^{-1})		$\Delta_H O^{=} M^{z+}$(aq) (kJ mol^{-1})	$\Delta_H O^{=} M^{z+}$(b) (kJ mol^{-1})
Mg^{2+}(o)	-134.60	-191.72	Mg^{2+}(b)	-134.60	-88.98
Fe^{2+}(o)	-18.04	-230.79	Fe^{2+}(b)	-182.04	-216.99
Al^{3+}(o)	-199.63	-251.75	Al^{3+}(b)	-199.63	-229.05
Fe^{3+}(o)	-242.74	-290.79	Fe^{3+}(b)	-242.74	-288.99
Ion H+	$\Delta_H O^{=} H^+$(o) (kJ mol^{-1})	Ion H^+	$\Delta_H O^{=} H^+$(b) (kJ mol^{-1})	Ion H^+	$\Delta_H O^{=} H^+$(e) (kJ mol^{-1})
H^+(i)	-249.58	H^+(d)	-311.98	H^+(e)	-287.20
K_{mixing} (Site I)	-0.857	K_{mixing} (Site M_2)	-0.579	K_{mixing} (Site M_3)	-0.108

[1] $\Delta_H O^{=} M^{z+}$(aq) values and references as reported in table 3 for the different cations

the oxygen atoms than those of ice II. This probably explains why the brucitic layer and the 2:1 layers are closely bonded in chlorites, thus forming a single structural unit. The outer and, to a less extent, the inner hydroxyl bonds (label e and o) located within the octahedral unit (1:1 and 2:1 layer, respectively) are less strongly bonded than in ice II, given the formation enthalpies obtained.

The set of parameters $\Delta_H O^{=} M^{z+}$(clay) is used to calculate the enthalpy of formation from constituent oxides (eq. 10), using equation (14). From enthalpies of oxides (table 3) and water in different states, the enthalpy of formation of a phyllosilicate can be evaluated (compare table 5) and compared with the Chermak and Rimstidt (1989) model. It can be seen that the present model gives better results for calibration phases belonging to the three families of phyllosilicates (fig. 2A**).** The high deviations observed for vermiculite and nontronite with the polyhedral model (-1.42 and -2%, respectively) are resolved with the present model. The improvement comes from a better consideration of the octahedral ferric iron, on the one hand and high tetrahedral aluminium content on the other hand.

Verifying the Model for Predicting the Enthalpy of Formation

With the prediction model developed here, enthalpies of formation of some verification phases listed in table 2 are calculated and are given in table 6 and compared with the polyhedral model (fig. 2B). For only one mineral, vermiculite, the enthalpy of formation predicted by using the electronegativity model is lower than -0.5 percent from the measured value. Globally, estimates by the Chermak and Rimstidt (1989) method display a wider range of discrepancies and a more important systematic deviation than the calculation performed by using the model developed here.

THE POLYHEDRAL DECOMPOSITION MODEL

Preliminary Aspects

A description of the method has already been given above (Statistical Methods section). The principle is to describe the thermodynamic functions as a linear combination of the mineral stoichiometric composition, including, in some cases,

TABLE 5

Predicted enthalpies of formation compared to the observed values for parameterization minerals

Minerals [1]	$\Delta H°_{f,obs}$ kJ/mol	$\Delta H°_{f,calc}$ kJ/mol	Err. kJ/mol	Err. (%)
10Å Pyrophyllite	-5640.00	-5635.77	-4.26	0.08
Talc	-5892.10	-5898.86	6.46	-0.11
Minnesotaite	-4822.99	-4822.27	0.03	0.00
Muscovite	-5974.80	-5960.15	-14.68	0.25
Paragonite	-5937.52	-5925.65	-11.87	0.20
Phlogopite	-6215.00	-6215.73	0.73	-0.01
Siderophylite	-5628.27	-5627.19	-1.08	0.02
Eastonite	-6348.94	-6336.12	-12.82	0.20
Annite	-5130.97	-5144.03	13.06	-0.25
Celadonite Al-Mg	-5834.74	-5844.41	9.67	-0.17
Celadonite Al-Fe	-5478.14	-5495.73	17.59	-0.32
Margarite	-6244.23	-6241.49	-2.74	0.04
Smectite MX80	-5656.37	-5651.24	-5.13	0.09
Illite IMt-2	-5711.25	-5711.22	-0.03	0.00
Nontronite Nau-1	-5035.69	-5035.87	0.18	0.00
Vermiculite SO	-6034.41	-6051.05	16.64	-0.28
14Å Clinochlore	-8909.59	-8887.97	-21.62	0.24
Chamosite	-7120.85	-7120.82	-0.03	0.00
Amesite	-9035.90	-9037.73	1.83	-0.02
Fe-Amesite	-7607.46	-7614.24	6.78	-0.09
Sudoite	-8655.25	-8647.76	0.78	-0.01
Chlorite Cca-2	-8240.14	-8234.47	-5.68	0.07
7Å Kaolinite	-4115.30	-4116.79	1.49	-0.04
Lizardite	-4362.00	-4365.23	3.23	-0.07
Antigorite	-71417.98	-71383.50	-34.48	0.05

[1] $\Delta H°_{f,obs}$ values and references as reported in table 1 for the different minerals

additional physical variables, such as volume for instance (Holland, 1989). The mineral structural formulas are decomposed into a sum of oxides and/or hydroxides of all cations, in such a way that the properties (ΔG^0_r, ΔH^0_r, ΔS^0_r, ΔV_r, ΔCp_r) of fictive solid-solid reactions are zero.

Mathematical formalism.—A simple mathematical description can be given, based on a matrix formalism. Considering a set of four phases (a, b, c and d) and the property X, and assuming that each of the four phases can be decomposed into three elementary polyhedrons (pol_1, pol_2 and pol_3), then the polyhedral decomposition consists in calculating the coordinates of each phase with respect to the three X_{pol} polyhedrons. In equation (21), the result of this calculation corresponds to the "Coordinates" matrix, which relates the matrix of the X mineral values, X_{min}, to the matrix of X for each polyhedron, $X_{pol.}$:

$$\begin{pmatrix} X_{min} \\ X^a_{min} \\ X^b_{min} \\ X^c_{min} \\ X^d_{min} \end{pmatrix} = \begin{pmatrix} & \text{Coordinates} & \\ c^a_1 & c^a_2 & c^a_3 \\ c^b_1 & c^b_2 & c^b_3 \\ c^c_1 & c^c_2 & c^c_3 \\ c^d_1 & c^d_2 & c^d_3 \end{pmatrix} \cdot \begin{pmatrix} X_{pol} \\ X_{pol1} \\ X_{pol2} \\ X_{pol3} \end{pmatrix} \qquad (21)$$

This relation implies that the number of mineral phases (a, b, c, d) is higher or equal to the number of polyhedrons (pol_1, pol_2, pol_3). The X_{pol} values are obtained by

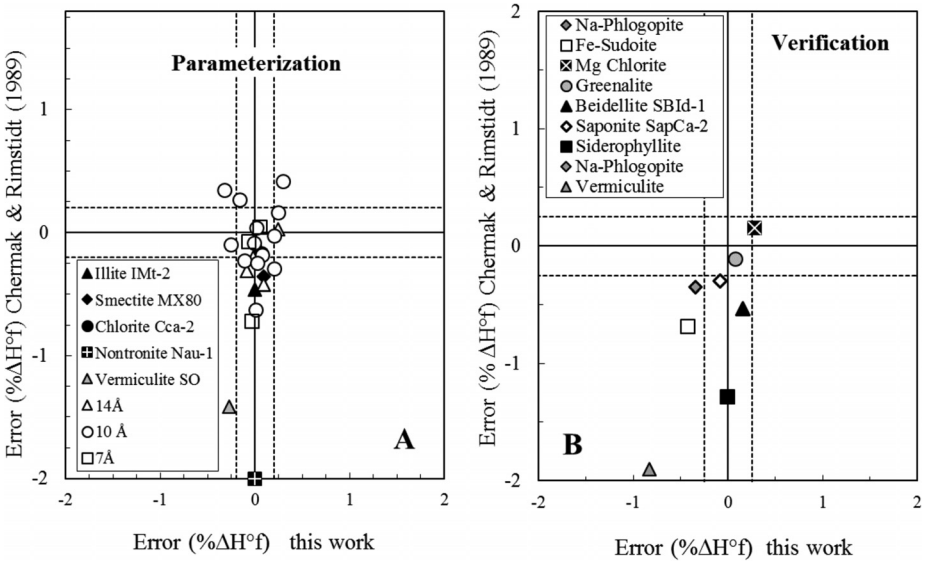

Fig. 2. Enthalpy of formation of phyllosilicates: comparison of the discrepancy of the estimates, calculated either with the present model or with the method of Chermak and Rimstidt (1989). (A) Parameterization phases; (B) Verification phases.

minimizing the squared difference between $X_{min(obs)}$ and $X_{min(calc)}$, which corresponds to the SSD (Sum of Squared Differences) parameter in the following equation:

$$SSD = \sum_{i=1}^{n} (X^i_{min}(obs) - X^i_{min}(calc))^2$$

with

$$X^i_{min}(calc) = \sum_{j=1}^{m} X_{polj} \cdot c^i_j \qquad (22)$$

Table 6

Predicted enthalpies compared to observed values for verification minerals

	Minerals [1]	$\Delta H°_{f,obs}$ kJ/mol	$\Delta H°_{f,calc}$ kJ/mol	Err. kJ/mol	Err. (%)
10 Å	Na-Phlogopite	-6172.57	-6193.68	21.11	-0.34
	Beidellite SBId-1	-5720.69	-5711.80	-8.89	0.16
	Saponite SapCa-2	-5994.40	-5999.26	4.86	-0.08
	Vermiculite	-5859.00	-5907.69	48.69	-0.83
	Siderophyllite	-5622.00	-5622.63	0.63	-0.01
14Å	Fe-Sudoite	-7912.77	-7946.67	33.90	-0.43
	Mg chlorite	-8744.20	-8719.39	-24.81	0.28
7Å	Greenalite	-3301.00	-3298.41	-2.59	0.08

[1] $\Delta H°_{f,obs}$ values and references as reported in table 2 for the different minerals

The minimization processes are carried out by adjusting the values of X_{polj} in order to minimize the SSD. The present model is applied to the properties S^{lat}, V, and for the $C_p(T)$ function, to each of the Maier-Kelley coefficients a, b and c.

Polyhedral decomposition.—The coordination polyhedra selected for the model are identical to those defined by Chermak and Rimstidt (1989). It should be mentioned that only a single polyhedral unit accounted for the FeIII contribution in their work. In addition, we could restore the symmetry of the model by integrating nontronite in the calibration and introducing a $Fe(OH)_3$ component into the model. In detail, the calculation of the coordinates is as follows:

— for tetrahedral sites, one considers complete disorder between sites (the same proportion of SiO_2 and Al_2O_3 between T_1 and T_2 sites),

— the interlayer space is considered as one single site,

— in the brucitic layer (for chlorites only), following Holland and others (1998) and Vidal and others (2005), Al first fills the M_4 site, then it fills the M_1 octahedral site. Finally, the remaining Al is equally distributed among the M_2 and M_3 sites.

For the 1:1 and 2:1 octahedral layer for the M_2+M_3 chlorite sites (the part not filled by Al), the distribution of cations $M^{z+}{}_i$ is calculated according to the relation:

$$\sum Z_i \cdot X_{OH}^{M_i^{z+}} = n_{OH}^{Clay} \tag{23}$$

and calculating a constant value for the ratio:

$$R = \frac{X_{Ox}^{M_i^{z+}}}{X_{OH}^{M_i^{z+}}} \tag{24}$$

for each cation $M^{z+}{}_i$. In these expressions, $X^i{}_{OH}$ is the $M^{z+}{}_i$ hydroxylated fraction and $X^i{}_{Ox}$ its oxide fraction. This process ensures an equal distribution of the elements among the octahedral sites. It also avoids calculating distributions where the total hydroxyl number could be different from the theoretical number (8, 2 and 4 for phyllosilicates 2:1:1, 2:1 and 1:1 respectively).

Parameterizing and Verifying the Model for Predicting S^{lat}, V and the Cp(T) Function

Parameterizing the polyhedral decomposition model.—The decomposition is applied to a list of 21 phyllosilicates from among the phases previously selected. From the list of the selected minerals (tables 1 and 6), none of the minerals whose properties were directly measured was discarded. However, the polyhedral decomposition model does not include specific interaction terms. Such terms would have been required in order to include the end members margarite and paragonite because of the existence of a miscibility gap with respect to muscovite (Roux and Hovis, 1996). The situation is similar for the celadonite end members that are not included either in the parameterization dataset because of their extreme octahedral charge. The results of the coordinate calculations are given in table 8, for the following oxides and hydroxides: $^{[8\text{-}12]}Na_2O$, $^{[8\text{-}12]}K_2O$, $^{[6\text{-}8]}CaO$, $^{[6]}Fe(OH)_3$, $^{[6]}Mg(OH)_2$, $^{[6]}Fe(OH)_2$, $^{[6]}Al(OH)_3$, $^{[6]}Al_2O_3$, $^{[6]}FeO$, $^{[6]}MgO$, $^{[6]}Fe_2O_3$, $^{[4]}Al_2O_3$, $^{[4]}SiO_2$ (the number in brackets indicates the coordination number of the component). The properties derived for each polyhedral unit are reported in table 5 and a comparison between predicted and observed values is provided in table 6. From the latter, the scattering of the discrepancies is quite homogeneous for the different properties and rather moderate.

Verification of the model for each property.—As for the enthalpy of formation, the verification is carried out using the rest of the minerals from tables 1 and 2, apart from the set used for model parameterization. For the entropy estimate, figure 3 compares the discrepancy with values estimated using either the present method or that of

TABLE 7

Polyhedral decomposition of the calibration minerals

	Minerals	$^{[8\text{-}12]}Na_2O$	$^{[8\text{-}12]}K_2O$	$^{[6\text{-}8]}CaO$	$^{6]}Fe(OH)_3$	$^{[6]}Mg(OH)_2$	$^{[6]}Fe(OH)_2$	$^{[6]}Al(OH)_3$	$^{[6]}Al_2O_3$	$^{[6]}FeO$	$^{[6]}MgO$	$^{[6]}Fe_2O_3$	$^{[4]}Al_2O_3$	$^{[4]}SiO_2$
10 Å	Muscovite		0.50					0.67	0.67				0.50	3.00
	Nontronite Nau-1		0.01	0.25	0.56	0.02		0.09	0.09		0.05	0.56	0.27	3.46
	Pyrophyllite							0.67	0.67					4.00
	Minnesotaite						1.00			2.00				4.00
	Phlogopite		0.50			1.00					2.00		0.50	3.00
	Talc					1.00					2.00			4.00
	Siderophyllite		0.50				0.57	0.29	0.36	1.43			1.00	2.00
	Illite IMt-2	0.02	0.38		0.10	0.08	0.03	0.49	0.47	0.06	0.16	0.10	0.31	3.39
	Smectite MX80	0.22	0.01	0.01	0.06	0.08	0.01	0.54	0.53	0.03	0.15	0.06	0.19	3.61
	Annite		0.5				1.00				2.00		0.50	3.00
	Eastonite		0.50			0.57		0.29	0.36		1.43		1.00	2.00
	Vermiculite SO			0.45	0.07	0.78	0.01	0.07	0.07	0.02	1.69	0.08	0.61	2.78
14 Å	Ripidolite CCa-2				0.10	1.38	0.79	1.12		0.92	1.59	0.06	0.68	2.63
	Amesite					2.17		1.22	0.39		1.83		1.00	2.00
	Sudoite					1.24		1.84	0.58		0.76		0.50	3.00
	Fe-Amesite						2.17	1.22	0.39	1.83			1.00	2.00
	Clinochlore					2.50		1.00			2.50		0.50	3.00
	Chamosite						2.50	1.00		2.50			0.50	3.00
7 Å	Kaolinite							1.33	0.33					2.00
	Antigorite					31.00					17.00			34.00
	Lizardite					2.00					1.00			2.00

TABLE 8

Thermodynamic properties of the polyhedral units

	S_i^{lat} J.mol^{-1}.K^{-1}	Cp (25°C) J.mol^{-1}.K^{-1}	a_i J.mol^{-1}.K^{-1}	b_i*10^3 J.mol^{-1}.K^{-2}	$-c_i*10^{-5}$ J.mol^{-1}.K	V_i cm^3.mol^{-1}
$^{[8-12]}Na_2O$	186.15	70.20	43.27	395.84	-80.98	22.97
$^{[8-12]}K_2O$	157.70	74.50	148.56	24.73	-72.39	27.26
$^{[6-8]}CaO$	133.08	42.43	63.88	315.36	-102.65	32.47
$^{[6]}Fe(OH)_3$	178.75	103.01	127.36	671.46	-199.61	24.98
$^{[6]}Mg(OH)_2$	61.12	72.19	71.47	66.54	-16.99	25.91
$^{[6]}Fe(OH)_2$	61.90	80.39	59.74	89.87	-5.46	21.61
$^{[6]}Al(OH)_3$	79.37	89.63	111.51	77.25	-39.92	34.96
$^{[6]}Al_2O_3$	55.02	74.89	299.02	-100.59	-172.58	4.91
$^{[6]}FeO$	55.74	42.35	141.77	-64.55	-71.27	10.59
$^{[6]}MgO$	27.89	30.84	131.03	-66.74	-71.38	4.57
$^{[6]}Fe_2O_3$	0.00	104.41	221.92	-515.68	32.22	14.23
$^{[4]}Al_2O_3$	29.42	80.91	-93.35	177.61	107.83	46.72
$^{[4]}SiO_2$	35.94	47.61	14.99	44.00	17.33	25.70

Bracketed numbers: correspond to the coordination number of the cation in the phyllosilicate structure

Holland (1989). For Holland (1989), we have considered it *a priori* the most effective method, including a contribution that depends on the molar volume. The method proposed here exhibits results that fall within the ± 5 percent domain, except for one point at −8.5 percent, which corresponds to the Mg-chlorite. For the Holland (1989) method (fig. 3), the discrepancies are larger, between +3 and -13 percent, and exhibit a clear systematic overestimation close to 5 percent, which has already been reported by Gailhanou and others (2013).

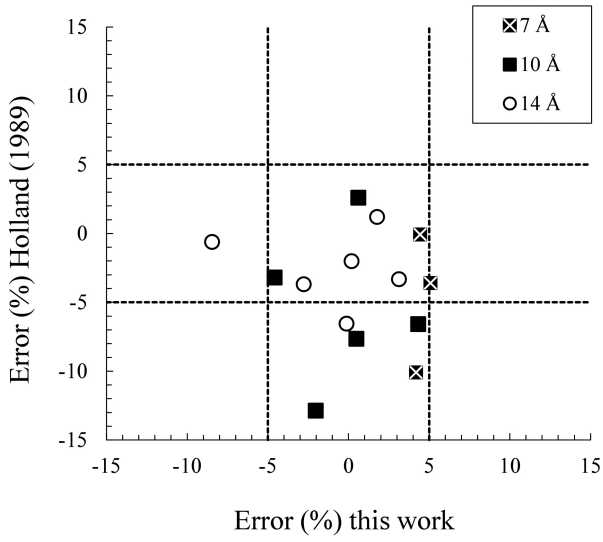

Fig. 3. Verification of the predicted entropy: comparison between two different estimating methods. Error (%) = (S^{lat}_{obs} - S^{lat}_{calc}) / S^{lat}_{obs} *100 ; S^{lat}_{obs} values and references as reported in table 1 for the different minerals.

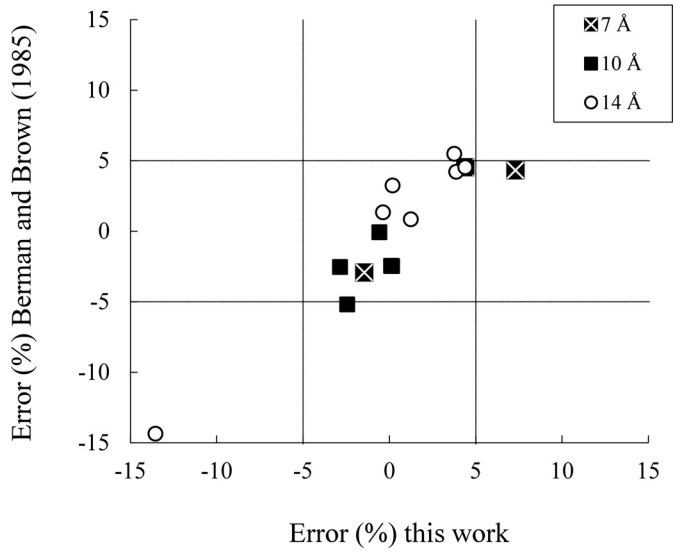

Fig. 4. Verification of the heat capacity predicted at room temperature Cp(25 °C): comparison between two different estimating methods.
Error (%) = $(Cp(25\ °C)_{obs} - Cp(25\ °C)_{calc}) / Cp(25\ °C)_{obs} * 100$; $Cp(25\ °C)_{obs}$ values and references as reported in table 1 for the different minerals.

The result of the Cp estimations at 25 °C is compared in figure 4 with data collected for this verification (table 2). The model shows a rather good agreement with experimental data, except for one point that accounts for the Fe-sudoite. Similarly to the Mg-chlorite previously, the thermodynamic properties of this arise from the work of Holland and Powell (1990, 1998). These inconsistencies may arise from the choice that we make to favor the selection from Vidal and others (2005) for chlorites. For the other minerals, the agreement is similar for the values predicted by the Berman and Brown (1985) method.

In figure 5, the full Cp(T) function predictions are compared with experimental data and with results from the Berman and Brown (1985) method. The agreement is, again, quite satisfactory. Temperature evolution of the predicted Cp follows the experimental trends and the 25 °C discrepancy does not tend to increase with temperature. In addition, the method proposed here provides similar or somewhat slightly better results than that of Berman and Brown (1985). Our improvement here is therefore to propose a method that consistently combines the prediction of all the main thermodynamic functions, for clay minerals, and which retains the same accuracy as the most efficient method for Cp(T) prediction.

A final comparison for the model prediction is reported in figure 6 for the molar volumes. We observe an excellent agreement between the model and the experimental measurements. To our knowledge, this work could be among the very few (if not the only) methods that enables the molar volumes of anhydrous clay minerals to be predicted.

EXTRAPOLATING CAPACITIES

Generally, predictive models are able to calculate the thermodynamic properties within the composition domain of the minerals used for the parameterization. This limitation may become a hindrance when considering alteration processes that release specific elements such as Cd, Ni, Zn or Li for example. Since such elements may be

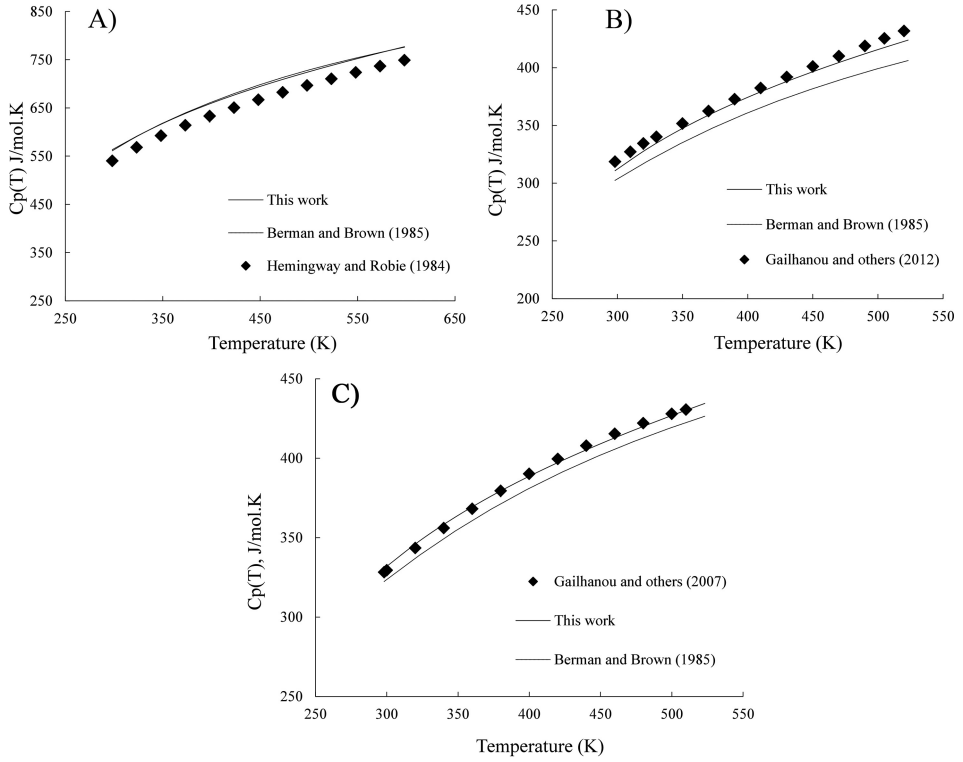

Fig. 5. Predicted Cp(T) functions, comparison with experimental data and the Berman and Brown (1985) method for the minerals (A) chamosite; (B) beidellite SBId-1; (C) illite IMt-2.

incorporated into the clay mineral structure, they may be irreversibly trapped but may also considerably modify the solubility of the phase. In addition, demonstrating such an ability increases the level of confidence concerning model predictions. Taking

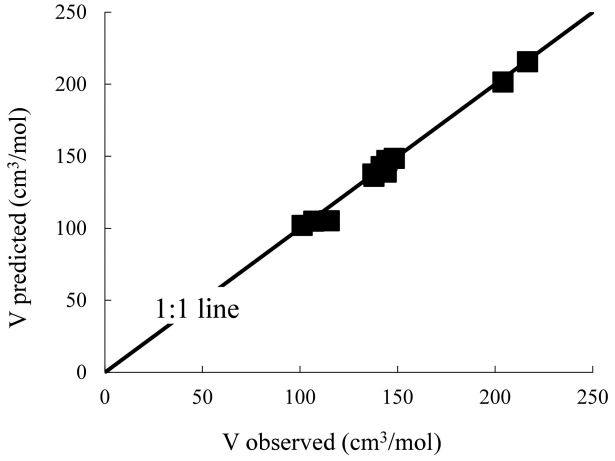

Fig. 6. Verification of the predicted molar volume. $V_{observed}$ values and references as reported in table 1 for the different minerals.

advantage of some recent calorimetric determinations on lithium-bearing phyllosilicates, we have extended the electronegativity scale concepts to the polyhedral method and tested the resulting approach.

The General Concept and Application to the Polyhedral Model

Globally, the idea is to develop parameters related to the clay structure that can also be calculated for aqueous cations. If a relation can be shown between aqueous cations and clay structure parameters, then it is possible to estimate the value for the element in the clay structure from its value for the aqueous cation. The method developed in the present work for the enthalpy of formation already includes such parameters ($\Delta O^{=}$ types). The following developments are carried out in order to propose similar parameters for the polyhedral model. A description of these developments for the enthalpy of formation is detailed by Vieillard (1994a).

If we express the fictive solution equilibrium with a basic polyhedral component M_xO_y as:

$$xM_{aq}^{z+} + yO^{=} = M_xO_y \tag{25}$$

and if we consider that the entropy of this fictive reaction is zero, we can define a $\Delta_S O^{=}$ parameter, corresponding to the entropy of the oxygen, as:

$$\Delta_S O^{=}(M_{ox}^{z+}) = S(O^{=}) = \frac{S(M_xO_y) - x \cdot S(M_{aq}^{z+})}{y} \tag{26}$$

Applying the same reasoning to the heat capacity or to the volume of basic polyhedral components, similar parameters can be defined for each of these properties:

$$\Delta_{Cp} O^{=}(M_{ox}^{z+}) = Cp(O^{=}) = \frac{Cp(M_xO_y) - x \cdot Cp(M_{aq}^{z+})}{y} \tag{27}$$

$$\Delta_{V,Cp} O^{=}(M_{ox}^{z+}) = \frac{V(M_xO_y) - x \cdot Cp(M_{aq}^{z+})}{y} \tag{28}$$

The latter is somewhat dubious since it associates heat capacity and volume in a final semi-empirical expression. However, this is the only way we have found to relate the molar volumes of the basic polyhedral components to those of the aqueous cations. For the sake of simplicity, the three Maier-Kelley coefficients are not considered here for the Cp(T) function. In that case, $\Delta_S O^{=}$ applies only to a constant value (at 25 °C or 298.15K).

The relations between the $\Delta O^{=}$ parameters are reported in figures 7A, 7B and 7C for the entropy, the heat capacity at 25 °C and the molar volume, respectively. For each of these properties, the correlation coefficient is quite high. For the volume term, the correlation is slightly less good (0.91).

From figures 7A, 7B and 7C are extracted the following relations:

$$\Delta_S O^{=} M^{z+}(\text{clay-inter.}) = 1.11 * \Delta_S O^{=} M^{z+(aq)} + 92.01 \tag{29}$$

$$\Delta_S O^{=} M^{z+}(\text{clay-tetr./octa.}) = 0.96 * \Delta_S O^{=} M^{z+}(aq) + 2.97 \tag{30}$$

$$\Delta_{Cp} O^{=} M^{z+}(\text{clay}) = 1.04 * \Delta_{Cp} O^{=} M^{z+}(aq) - 4.03 \tag{31}$$

$$\Delta_{V,Cp} O^{=} M^{z+}(\text{clay}) = 1.06 * \Delta_{V,Cp} O^{=} M^{z+}(aq) - 4.30 \tag{32}$$

The parameters $\Delta_S O^{=} M^{z+}(aq)$, $\Delta_{Cp} O^{=} M^{z+}(aq)$ and $\Delta_{V,Cp} O^{=} M^{z+}(aq)$ are calculated from relations (26) to (28), with thermodynamic properties from the aqueous ions

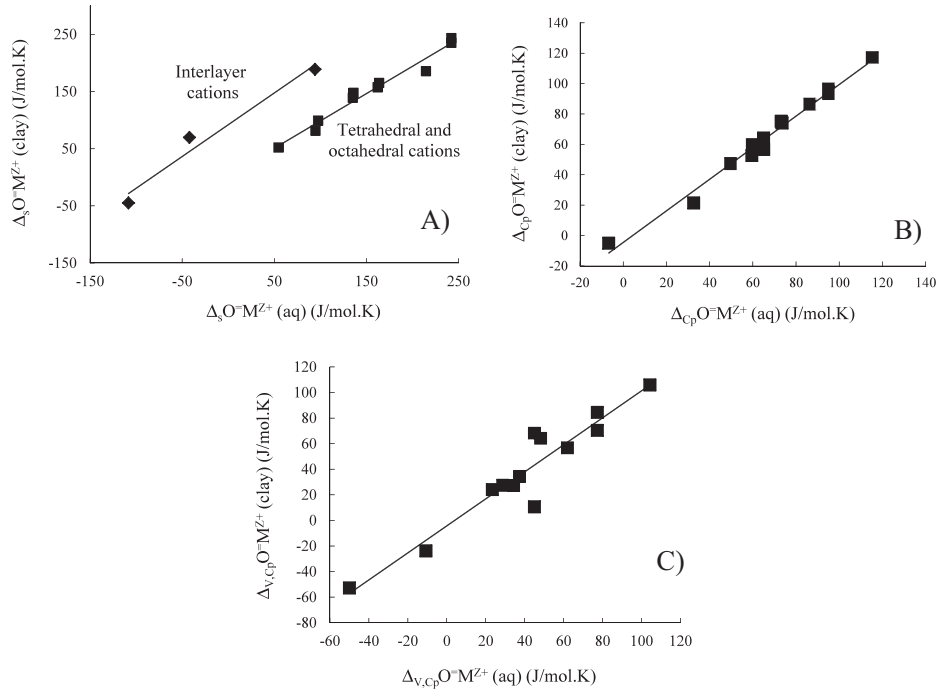

Fig. 7. Development of predictive capacity for (A) entropy, (B) heat capacity at 25 °C and (C) volume estimates, respectively.

from the Thermochimie database (table 3, same references for entropies). Then, using relations (29) to (32), the parameters $\Delta_S O^{=}M^{z+}$(clay), $\Delta_{Cp} O^{=}M^{z+}$(clay) and $\Delta_{V,Cp} O^{=}M^{z+}$(clay) are calculated. The results are reported in table 7 where the relations (26) to (28) are finally reversed in order to obtain the thermodynamic properties of the polyhedral units.

Application to the Prediction of Enthalpy

For enthalpies of formation, values of the parameters $\Delta_H O^{=} M^{z+}$(clay) obtained in the minimization procedure of enthalpy of formation developed previously are plotted in figure 8 versus $\Delta_H O^{=} M^{z+}$(aq) (eq.18), and provide four relationships depending on the nature of the site:

$$\text{Interlayer sites: } \Delta_H O^{=} M^{z+}(l) = 99.06 + 2.18*[\Delta_H O^{=} M^{z+}(aq)] + 2.57\ 10^{-3}*[\Delta_H O^{=} Mz+(aq)]^2 \quad (33)$$

$$\text{Tetrahedral sites: } \Delta_H O^{=} M^{z+}(t) = -76.67 + 0.97*[\Delta_H O^{=} M^{z+}(aq)] \quad (34)$$

$$\text{Octahedral sites: } \Delta_H O^{=} M^{z+}(o) = -72.23 + 0.89*[\Delta_H O^{=} M^{z+}(aq)] \quad (35)$$

$$\text{Brucitic sites: } \Delta_H O^{=} M^{z+}(b) = 141.31 + 1.83*[\Delta_H O^{=} M^{z+}(aq)] \quad (36)$$

From relations (33) to (36), the parameter $\Delta_H O^{=} M^{z+}$(clay) in the four different sites (tetrahedral, octahedral, octahedral and brucitic) can be evaluated from the parame-

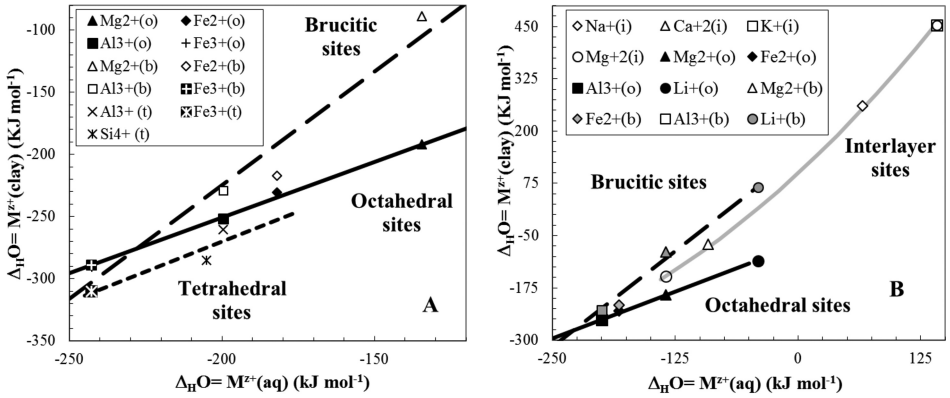

Fig. 8. Relationship between $\Delta_H O^{=}M_{i,clay^{z_i}}+$ and $\Delta_H O^{=}M_{i,aq}^{z_i+}$ for cations in the interlayer, octahedral and brucitic sites.

ter $\Delta_H O^{=}M^{z+}(aq)$ in the aqueous state directly obtained from the enthalpy of formation of the oxide and the aqueous cations from equations (10-14). The results of such a calculation are reported in table 11 for a large set of elements, taking into account the possible locations into the interlayer, octahedral or brucitic sites. Then, from the previous result, the standard enthalpy of formation can be directly computed from (eq. 9), as realized for Li-bearing phyllosilicates, in the following section.

An Evaluation of the Extrapolating Capacities: The Case of Lithium-Bearing Phyllosilicates

Considerable efforts to acquire the thermodynamic properties of some lithium-bearing phyllosilicates have been made recently and have been summarized by Ogorodova and others (2010). In this work, the authors have considered Li-bearing minerals belonging to the mica or the brittle micas family, including variable amounts of iron and fluorine.

The enthalpy of formation has been acquired for 12 of these mica phases, by drop calorimetry in lead borate solvent at high temperature. In addition, the heat capacity of 6 phases has been measured by low temperature adiabatic calorimetry, providing the heat capacity function and the entropy. The composition of the phases includes some minor amounts of Ti, Mn, Cs, Rb and above all, large amounts of Li and F (replacing the hydroxyl groups). In addition, a complete set of thermodynamic properties has been measured on a Li-bearing berthierine by Blanc and others (2014) including the formation enthalpy and the entropy. It has been included in the set of Li-bearing phyllosilicates for this verification.

The entropy and heat capacity (25 °C) has been predicted for the 7 minerals whose properties were directly measured and also for the 4 theoretical end-members. The estimates include the contributions of Ti, Mn, Cs, Rb and Li, calculated by coupling the polyhedral model with the electronegativity ($\Delta O^{=}$) approach, as developed in the previous section. Unfortunately, the influence of OH/F substitution cannot be assessed directly. This was finally achieved by considering a fictive exchange reaction between fluorophlogopite and hydroxylphlogopite, whose thermodynamic properties are provided by Robie and Hemingway (1995). The results are reported and compared with experimental data in figures 9A and 9B. For figure 9A, the results from the present method can be compared with another estimation method that includes the contribution of lithium. Such methods could not be found for heat capacity.

Generally speaking, it can be said that both methods display a similar scattering range. This is already quite satisfactory in our case, since no Li-bearing minerals were

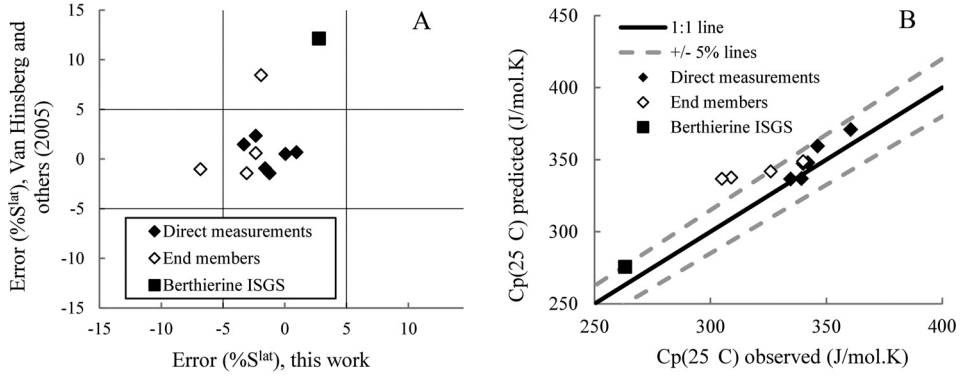

Fig. 9. Comparison between experimental and predicted properties of some lithium-bearing micas. Results for (A) entropy and (B) heat capacity at 25 °C.

included in our parameterization set of minerals. In detail, this range is extended, for the method of Van Hinsberg and others (2005a, 2005b), because of two samples that display an iron content greater than 1.0 cations per $O_{10}(OH)_2$. This somewhat limits the application range, since Fe is quite a common element in phyllosilicate structures. For the method developed here, the scattering range is extended by one point that refers to the Li-richest phyllosilicate, polylithionite, with 2.0 Li per $O_{10}(OH)_2$. Below 1.68 Li, the scattering range remains within the usual ±5 percent limit. This should indicate that, when reaching extreme composition, the extrapolation ability of the model developed here is less accurate. Also, this point seems less difficult to manage than the failure of the alternative method (Van Hinsberg and others, 2005b) to take into account Fe-rich compositions. The results shown in figure 9B indicate a satisfactory agreement of the calculations with the experimental data, close to the limits (± 5%) previously defined when verifying the model (figs. 4 and 5).

A similar comparison had been made for the enthalpy of formation of the Li-bearing minerals, including the theoretical end-members and berthierine. In order to take into account the fluorine contribution, we have also calculated the enthalpy of the fictive exchange reaction F/OH, between fluorophlogopite and hydroxylphlogopite from Robie and Hemingway (1995), which gives a value of 81 kJ mol^{-1}.The difference between predicted and measured enthalpy of formation of Li-bearing phyllosilicates provide a range between -1.0 and +2.0 percent, better than that obtained using the method of Van Hinsberg and others (2005a). In addition, the latter implies a global overestimate (in absolute value) close to 2.0 percent (fig. 10).

Finally, the extrapolating capacities demonstrated by our predictive model display some interesting abilities and compares favorably even with methods that already include the element of interest in their parameterization set of minerals.

UNCERTAINTY ISSUES

From the previous results, it appears that the uncertainty ranges related to the estimates depend on the property considered and on the data used to assess the performance of the models. For the entropy and heat capacity estimates, the case is quite simple, as displayed in figures 3, 4, 9A and 9B. Generally speaking, S^{lat} and Cp(25 °C) predictions fall within an uncertainty interval of ±5 percent. In the case of vermiculite, this corresponds, through eq. (1), to a contribution to the Gibbs free energy uncertainty of ±4.5 kJ/mol.

For the prediction of the enthalpy of formation, different cases need to be distinguished. The largest uncertainty range is found for the extrapolating capacity

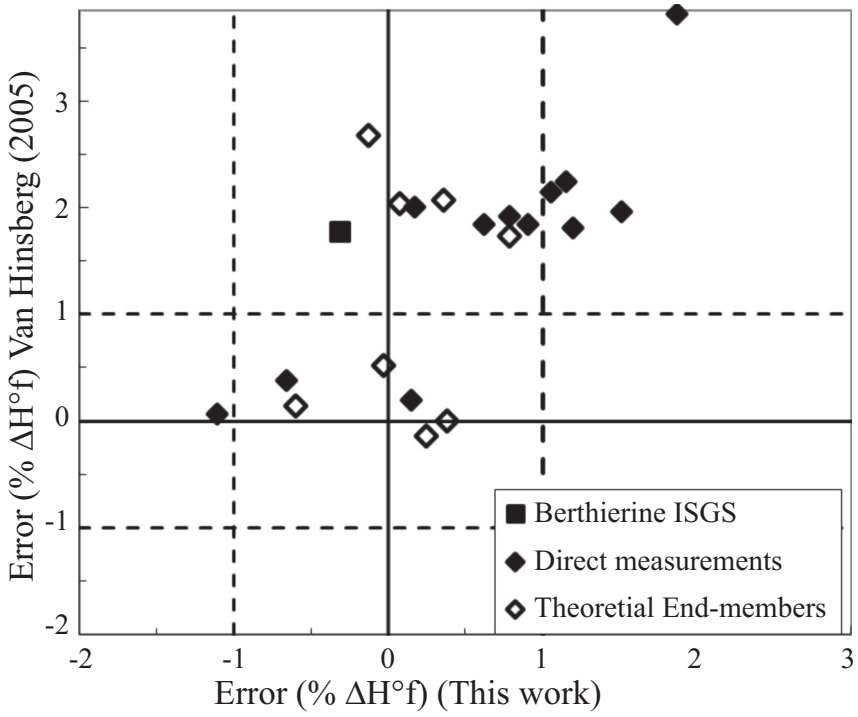

Fig. 10. Comparison between experimental and predicted formation enthalpy of some lithium-bearing micas.

with ±1.5 percent or ±90kJ/mol for vermiculite at 25 °C, which is important. For verification minerals (fig. 2B and table 6), the uncertainty is reduced to ±0.5 percent or ±30kJ/mol for vermiculite. This interval is still large but greatly reduced with respect to the previous one. From figure 10, it is possible that part of the extent of this interval stems not only from the inadequacy of the estimation method but also from a relative scattering of the experimental data. From tables 5 and 6, collation of the low-temperature dissolution calorimetry data gives an uncertainty interval of ±0.15 percent or ±10 kJ/mol. This method has been discussed by Blanc and others (2013) as being especially well suited to the measurement of the enthalpy of formation of clay minerals. A reasonable uncertainty interval could be found by averaging the two last intervals, which gives the value ±0.33 percent or ±20 kJ/mol for vermiculite, for instance.

Taking into account only low temperature dissolution calorimetry data could have led to a reduction in such an uncertainty interval. Unfortunately, no other data of this type could be gathered from previously published works.

Combining the predictive models: Gibbs free energy estimates

Estimating the Gibbs free energy is an important step since it finally makes it possible to predict the equilibrium constant of any clay mineral end-member by using equations (5) and (6). Indeed, the LogK(T) function is then introduced into a thermodynamic database in order to enable geochemical calculations. Once the Gibbs energy estimates have been verified, a complete database can be provided for the clay mineral end-members. Finally, a simple and final verification step consists in calculat-

TABLE 9

Parameterization of the polyhedral model: results for entropy, heat capacity and volume

	Minerals [1]	S^{lat}_{obs}	S^{lat}_{calc}	Err.(%)	$Cp(25°C)_{obs}$	$Cp(25°C)_{calc}$	Err.(%)	V_{obs}	V_{calc}	Err(%)
10 Å	Muscovite	287.70	290.97	-1.13	326.00	330.21	-1.28	140.81	140.68	0.09
	Nontronite Nau-1	282.73	281.80	0.33	335.15	332.51	0.79	136.38	136.29	0.06
	Pyrophyllite	239.40	233.35	2.56	293.76	300.12	-2.14	128.10	129.39	-1.00
	Minnesotaite	310.66	317.13	-2.06	364.40	355.53	2.46	148.50	145.61	1.97
	Phlogopite	315.90	318.27	-0.75	354.65	354.40	0.07	149.65	149.14	0.34
	Talc	260.80	260.65	0.06	321.77	324.31	-0.79	136.20	137.85	-1.21
	Siderophyllite	337.64	337.47	0.05	363.17	372.17	-2.45	150.63	150.98	-0.23
	Illite IMt-2	289.59	291.98	-0.82	328.20	330.94	-0.83	139.18	139.70	-0.37
	Smectite MX80	274.26	274.02	0.09	322.74	318.00	1.48	134.92	134.86	0.04
	Annite	383.88	374.75	2.41	390.31	385.62	1.21	154.30	156.89	-1.67
	Eastonite	295.40	297.24	-0.62	350.95	351.04	-0.02	147.51	144.82	1.84
	Vermiculite SO	295.37	295.89	-0.18	346.39	337.83	2.50	148.36	148.41	-0.03
14 Å	Chlorite CCa-2	443.29	450.35	-1.58	547.02	548.59	-0.29	211.93	211.89	0.02
	Amesite	403.20	403.26	-0.01	540.47	527.75	2.38	205.20	207.27	-1.00
	Sudoite	390.50	397.47	-1.77	509.72	504.58	1.01	205.10	203.24	0.91
	Fe-Amesite	461.27	456.01	1.15	564.28	566.61	-0.41	209.00	209.00	0.00
	Clinochlore	435.15	424.42	2.50	516.34	530.49	-2.70	211.47	211.61	-0.07
	Chamosite	492.49	495.99	-0.71	574.75	579.76	-0.87	215.88	215.93	-0.02
7 Å	Kaolinite	200.90	196.05	2.45	243.37	239.69	1.52	99.34	99.66	-0.32
	Antigorite	3591.00	3590.78	0.01	4380.66	4381.03	-0.01	1754.80	1754.71	0.01
	Lizardite	216.30	222.01	-2.60	274.15	270.45	1.36	107.50	107.79	-0.27

[1] S^{lat}_{obs}, $Cp(25\ °C)_{obs}$ and V_{obs} values and references as reported in table 1 for the different minerals

ing the stability fields of those minerals with respect to the other phases, using the newly created database, in order to check phase relations in predominance diagrams.

Estimating the Gibbs free energy for phyllosilicates.—By combining the estimates of the enthalpy of formation and the entropy through equations (1) and (2), it is possible to predict the Gibbs free energy values. Since the accuracy of predictions for ΔH^0_f and S^{lat} have already been checked, the main question arises from the additional entropy terms S^{mag} and S^{conf}. For chamosite for example, table 1 indicates that S^{mag} reaches 66.91 J/mol.K. This contributes up to -20 kJ/mol to the final value of ΔG^0_f and modifies it by -0.28 percent. Such modification is far from negligible and has to be tested. Calculations were performed by combining S^{mag} and S^{conf} from tables 1 and 2 and the estimates from tables 5, 6 and 9. In tables 12 and 13 and figures 11A and 11B, the results are compared to the experimentally measured ΔG^0_f values from tables 1 and 2.

From tables 12 and 13 and figures 11A and 11B, it is clear that introducing the configurational and magnetic entropy terms does not significantly increase the discrepancies with respect to experimental data. These remain of the same order of magnitude as discrepancies observed for ΔH^0_f predictions (tables 5 and 6). In fact, for the verification minerals, figure 2 indicates a general and small overestimate of ΔH^0_f whereas S^{lat} in figure 3 is slightly underestimated. Finally, the combination tends to reduce the overall uncertainty for ΔG^0_f estimates.

Based on the estimation models developed previously, the thermodynamic properties of several end-members has been calculated in order to propose a database for clay minerals with ideal compositions (table 14) in order to be included into more general geochemical databases (Blanc and others 2012; Giffaut and others 2014). The compositions of the clay end-members has been chosen in order to cover a large domain, including illite and smectite (di- and trioctahedral), Al/Fe/Mg substitutions

TABLE 10

S^{lat}, Cp (25 °C) and V values of the polyhedral units for different ions located in the interlayer and octahedral sites

	Interlayer sites				Octahedral sites		
Oxide/ Hydroxide	S^{lat}(Clay) J.mol^{-1}.K^{-1}	Cp(25°C, Clay) J.mol^{-1}.K^{-1}	V(Clay) cm^3.mol^{-1}	Oxide/ Hydroxide	S^{lat}(Clay) J.mol^{-1}.K^{-1}	Cp(25°C, Clay) J.mol^{-1}.K^{-1}	V(Clay) cm^3.mol^{-1}
Cs_2O	226.01	77.12	62.25	MnO	57.15	42.52	10.72
BaO	171.12	47.38	25.92	$Mn(OH)_2$	81.74		21.29
SrO	157.10	44.90	20.19	TiO_2	44.36	51.75	15.24
Li_2O	131.43	47.48	4.26	Cr_2O_3	56.30	120.76	29.55
MnO	165.74	42.52	10.72	$Cr(OH)_3$	85.95		27.96
CuO	150.06	37.67	5.19	NiO	33.03	45.70	7.01
CoO	162.43	42.35	9.95	$Ni(OH)_2$	42.59	116.19	15.00
NiO	148.05	45.70	7.01	CoO	48.60	42.35	9.95
CdO	160.85	41.95	13.11	$Co(OH)_2$	91.10		19.65
ZnO	152.54	36.72	8.65	ZnO	39.79	36.72	8.65
H_2O	169.65	74.33	14.85	$Zn(OH)_2$	79.65	65.76	23.50
Al_2O_3	406.90	80.98	30.53	Li_2O	40.80	47.48	4.26
Rb_2O	204.83	73.99	46.40	LiOH	45.04	45.38	9.51
MgO	136.99	35.59	8.97				

in the octahedral sheet and 4 interlayer compositions (Na, K, Ca and Mg). For chlorites, the present models have been developed consistently with Vidal and others (2005) work. The latter already proposed end-member compositions that make it

TABLE 11

Values of the parameter $\Delta_H O^{=} M^{z+}$ (clay) calculated for different ions located in interlayer, and octahedral sites

Cation	Interlayer site $\Delta_H O^{=} M^{z+}$(i) kJ mol^{-1}	Octahedral $\Delta_H O^{=} M^{z+}$(o) (kJ mol^{-1})	Brucitic site $\Delta_H O^{=} M^{z+}$(b) kJ mol^{-1}
Cs^+	544.22		
Ba^{2+}	70.57		
Sr^{2+}	15.35		
Li^+	14.24	-108.79	66.34
Mn^{2+}	-189.17	-218.94	-159.60
Cu^{2+}	-256.22		
Co^{2+}	-208.92	-232.59	-187.60
Ni^{2+}	-215.73	-237.50	-197.67
Cd^{2+}	-212.38		
Zn^{2+}	-222.87	-242.78	-208.49
H_3O^+	-310.00		
Al^{3+}	-232.84		
Rb^+	522.89		
Mg^{2+}	-147.25		
Cr^{3+}		-243.61	-210.19
Ti^{4+}		-291.05	-307.49
NH_4^+	171.85		

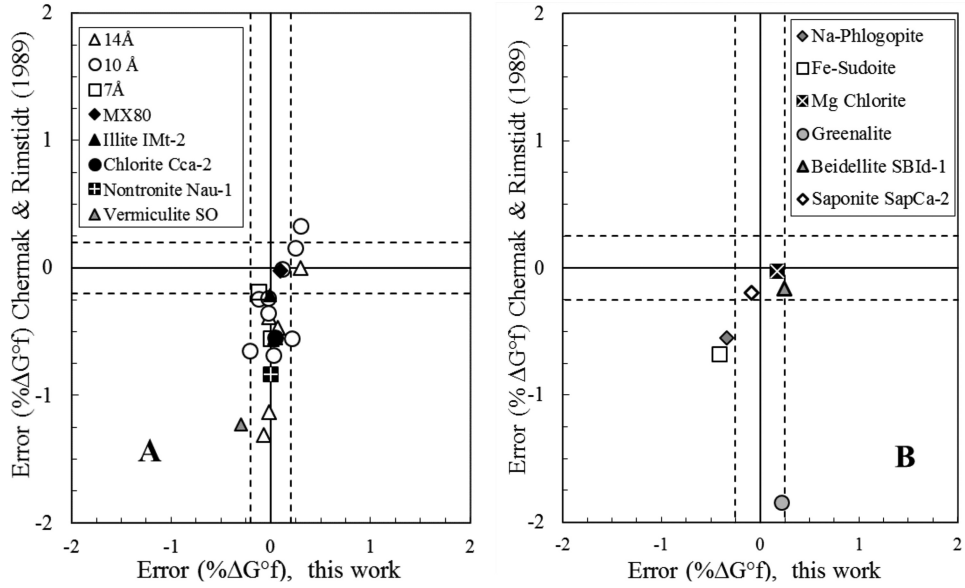

Fig. 11. Predicted ΔG^0_f for phyllosilicates: comparison of the discrepancy between experimental measurements and values calculated either with the present model or with the method of Chermak and Rimstidt (1989). (A) Phases for parameterization; (B) Verification phases.

possible to take into account a large composition domain and the present work relies on the thermodynamic properties refined by Vidal and others (2005) for such phases. For the 7Å phases, we have estimated the properties of a cronstedtite and a berthierine. These stand for the extreme transformation products of a smectite in contact with iron, as determined by Mosser-Ruck and others (2010).

Based on the values calculated in table 14 and on S^{conf} and S^{mag} from the Ulbrich and Waldbaum (1976) method, the equilibrium constant was calculated for each end-member and predominance diagrams could be drawn in various chemical systems. This exercise makes it possible to check the consistency of the clay mineral stability domains, with respect to themselves and with respect to minerals other than phyllosilicates. Among these, zeolites play an important role in limiting clay mineral stability fields in the highly alkaline or calc-alkaline part of the stability diagrams. In Appendix 2, a selection for the thermodynamic properties of the main zeolite minerals is proposed. The activity diagrams displayed in figures 12, 13 and 14 makes it possible to test the stability field of the clay mineral end–members from table 14 but also, as a secondary goal, the stability domains of zeolite mineral, calculated using the thermodynamic properties reported in Appendix 2. The stability domains are calculated by combining the mass action laws (eq. 7) for two minerals (univariant line) or for three minerals (invariant points), using equilibrium constants calculated from the thermodynamic properties predicted or selected in this work (table 1, table 14 and Appendix 2) and implemented into equation 1, in order to calculate the Gibbs energies at T and P of interest.

In figure 12 are displayed the stability diagrams in the chemical system SiO_2-Al_2O_3-MgO-K_2O-Na_2O-H_2O, at 25 and 150 °C. For the potassic sub-systems, figure 12A presents a conventional configuration of the stability fields. Beidellite is intercalated between illite and pyrophyllite instead of montmorillonite since, because of the compositions retained in table 14, the latter includes a quantity of magnesium. Indeed,

TABLE 12

Assessment of the free enthalpy predictions for the parameterization set of minerals

	Minerals [1]	$\Delta H°_{f,est}$ kJ.mol^{-1}	S^{lat}_{est} J.mol^{-1}.K^{-1}	$S^{mag}+S^{conf}$ J.mol^{-1}.K^{-1}	$\Delta G°_{f,est.}$ kJ.mol^{-1}	$\Delta G°_{f,meas}$ kJ.mol^{-1}	Err. %
10 Å	Pyrophyllite	-5635.77	233.17	0.00	-5260.03	-5266.11	0.12
	Talc	-5898.86	260.76	0.00	-5518.99	-5512.24	-0.12
	Minnesotaite	-4822.27	317.20	40.14	-4476.02	-4474.75	-0.03
	Muscovite	-5960.15	290.80	18.70	-5585.05	-5598.77	0.25
	Paragonite	-5925.65	305.31	18.70	-5558.87	-5562.32	0.06
	Phlogopite	-6215.73	318.39	18.70	-5836.51	-5835.03	-0.03
	Siderophyllite	-5627.19	337.48	37.36	-5260.91	-5262.04	0.02
	Eastonite	-6336.12	297.27	10.60	-5946.66	-5958.92	0.21
	Annite	-5144.03	374.83	40.14	-4792.84	-4782.49	-0.22
	Smectite MX80	-5651.24	273.10	28.59	-5288.20	-5293.40	0.10
	Illite IMt-2	-5711.83	290.41	36.83	-5345.86	-5345.20	-0.01
	Nontronite Nau-1	-5035.87	273.53	58.36	-4684.77	-4684.79	0.00
	Vermiculite SO	-6051.05	294.78	31.46	-5683.14	-5666.17	-0.30
14Å	Clinochlore	-8887.97	424.75	0.00	-8229.29	-8250.58	0.30
	Chamosite.	-7120.82	496.17	66.91	-6511.42	-6506.86	-0.02
	Amesite	-9037.73	403.47	0.00	-8367.75	-8365.84	-0.02
	Fe-Amesite	-7614.24	456.07	53.53	-6982.33	-6977.06	-0.07
	Sudoite	-8647.76	397.62	0.00	-7989.91	-7995.30	0.07
	Ripidolite	-8234.47	449.23	27.60	-7590.38	-7593.37	0.05
7Å	Kaolinite	-4116.79	196.16	0.00	-3794.01	-3793.94	0.00
	Lizardite	-4365.23	222.00	0.00	-4037.81	-4032.88	-0.12
	Antigorite	-71383.50	3590.77	0.00	-66092.33	-66126.88	0.05

[1] $\Delta G°_{f,meas}$ values and references reported in table 1 for the different minerals

as long as magnesium is allowed in the system, montmorillonite largely replaces beidellite, as shown in figures 12C and 12D. The temperature increase also produces a phillipsite to microcline transition, which is quite correct with respect to the experiments carried out by Chermak (1993) on an Opalinus Clay sample altered by alkaline solutions. The same trend can be found for the sodic sub-system in figures 12E to 12F. The introduction of magnesium in figure 12C and figure 12D allows vermiculite to appear, along with saponite and clinochlore. Temperature implies an increase in the vermiculite and clinochlore stability fields, at the expense of saponite and montmoril-

TABLE 13

Assessment of the free enthalpy predictions for verification minerals

	Verification Minerals [1]	$\Delta H°_{f,est}$ kJ.mol^{-1}	S^{0}_{est} J.mol^{-1}.K^{-1}	$S^{mag}+S^{conf}$ J.mol^{-1}.K^{-1}	$\Delta G°_{f,est.}$ kJ.mol^{-1}	$\Delta G°_{f,meas}$ kJ.mol^{-1}	Err. %
10 Å	Na-Phlogopite	-6193.68	332.90	0.00	-5817.19	-5791.64	-0.44
	Beidellite SBId-1	-5711.80	258.43	23.66	-5344.93	-5357.92	0.24
	Saponite SapCa-1	-5999.26	294.65	18.11	-5628.95	-5624.22	-0.08
14Å	Fe-Sudoite	-7946.67	416.96	26.76	-7305.78	-7275.84	-0.44
	Mg-Chlorite	-8719.39	444.00	0.00	-8064.55	-8078.63	0.17
7Å	Greenalite	-3298.41	251.26	40.14	-2996.50	-3003.00	0.22

[1] $\Delta G°_{f,meas}$ values and references reported in table 2 for the different minerals

TABLE 14

Predicted values for the thermodynamic properties of clay mineral end-members

Mineral		Formula	ΔH^0_f kJ.mol^{-1}	S^{lat} J.mol^{-1}.K^{-1}	$S^{conf}+S^{mag}$ J.mol^{-1}.K^{-1}	Cp (25°C) J.mol^{-1}.K^{-1}	V° cm^3.mol^{-1}
Montmorillonite	(MgK)	$K_{0.34}Mg_{0.34}Al_{1.66}Si_4O_{10}(OH)_2$	-5703.51	260.13	12.91	311.33	134.69
Low-charge	(MgNa)	$Na_{0.34}Mg_{0.34}Al_{1.66}Si_4O_{10}(OH)_2$	-5690.41	264.97	12.91	310.60	133.96
	(MgCa)	$Ca_{0.17}Mg_{0.34}Al_{1.66}Si_4O_{10}(OH)_2$	-5690.29	255.94	12.91	305.88	135.58
	(MgMg)	$Mg_{0.17}Mg_{0.34}Al_{1.66}Si_4O_{10}(OH)_2$	-5676.01	256.61	12.91	304.71	131.58
Montmorillonite	(HcK)	$K_{0.6}Mg_{0.6}Al_{1.4}Si_4O_{10}(OH)_2$	-5757.74	280.59	15.75	319.96	138.75
High-charge	(HcNa)	$Na_{0.6}Mg_{0.6}Al_{1.4}Si_4O_{10}(OH)_2$	-5734.63	289.13	15.75	318.67	137.47
	(HcCa)	$Ca_{0.3}Mg_{0.6}Al_{1.4}Si_4O_{10}(OH)_2$	-5734.42	273.21	15.75	310.34	140.32
	(HcMg)	$Mg_{0.3}Mg_{0.6}Al_{1.4}Si_4O_{10}(OH)_2$	-5709.22	274.38	15.75	308.29	133.27
Saponite	(K)	$K_{0.34}Mg_3Al_{0.34}Si_{3.66}O_{10}(OH)_2$	-6010.39	280.25	13.71	334.54	141.69
	(Na)	$Na_{0.34}Mg_3Al_{0.34}Si_{3.66}O_{10}(OH)_2$	-5997.76	285.09	13.71	333.81	140.96
	(Ca)	$Ca_{0.17}Mg_3Al_{0.34}Si_{3.66}O_{10}(OH)_2$	-5998.44	276.07	13.71	329.09	142.57
	(Mg)	$Mg_{0.17}Mg_3Al_{0.34}Si_{3.66}O_{10}(OH)_2$	-5984.34	276.73	13.71	327.93	138.58
Saponite- Fe	(FeK)	$K_{0.34}Mg_2Fe^{+2}Al_{0.34}Si_{3.66}O_{10}(OH)_2$	-5645.53	299.08	42.96	344.95	144.27
	(FeNa)	$Na_{0.34}Mg_2Fe^{+2}Al_{0.34}Si_{3.66}O_{10}(OH)_2$	-5633.89	303.91	42.96	344.23	143.54
	(FeCa)	$Ca_{0.17}Mg_2Fe^{+2}Al_{0.34}Si_{3.66}O_{10}(OH)_2$	-5633.57	294.89	42.96	339.50	145.15
	(FeMg)	$Mg_{0.17}Mg_2Fe^{+2}Al_{0.34}Si_{3.66}O_{10}(OH)_2$	-5619.48	295.56	42.96	338.33	141.16
Nontronite	(K)	$K_{0.34}Fe^{+3}{}_{1.67}Al_{0.67}Si_{3.66}O_{10}(OH)_2$	-4994.27	277.64	46.02	334.23	132.85
	(Na)	$Na_{0.34}Fe^{+3}{}_{1.67}Al_{0.67}Si_{3.66}O_{10}(OH)_2$	-4981.64	282.47	46.02	333.50	132.12
	(Ca)	$Ca_{0.17}Fe^{+3}{}_{1.67}Al_{0.67}Si_{3.66}O_{10}(OH)_2$	-4982.32	273.45	46.02	328.78	133.74
	(Mg)	$Mg_{0.17}Fe^{+3}{}_{1.67}Al_{0.67}Si_{3.66}O_{10}(OH)_2$	-4968.22	274.12	46.02	327.62	129.74
Beidellite	(K)	$K_{0.34}Al_{2.34}Si_{3.66}O_{10}(OH)_2$	-5749.86	252.94	13.71	310.35	133.22
	(Na)	$Na_{0.34}Al_{2.34}Si_{3.66}O_{10}(OH)_2$	-5737.23	257.78	13.71	309.62	132.49
	(Ca)	$Ca_{0.17}Al_{2.34}Si_{3.66}O_{10}(OH)_2$	-5737.91	248.76	13.71	304.90	134.10
	(Mg)	$Mg_{0.17}Al_{2.34}Si_{3.66}O_{10}(OH)_2$	-5723.81	249.42	13.71	303.74	130.11
Illite	(Mg)	$K_{0.85}Mg_{0.25}Al_{2.35}Si_{3.4}O_{10}(OH)_2$	-5881.39	287.62	18.66	326.41	140.06
	(FeII)	$K_{0.85}Fe^{+2}{}_{0.25}Al_{2.35}Si_{3.4}O_{10}(OH)_2$	-5796.29	292.22	22.01	329.00	140.67
	(FeIII)	$K_{0.85}Fe^{+3}{}_{0.25}Al_{2.6}Si_{3.15}O_{10}(OH)_2$	-5795.39	286.03	22.07	329.28	138.92
	(Al)	$K_{0.85}Al_{2.85}Si_{3.15}O_{10}(OH)_2$	-5913.65	282.33	12.08	325.70	138.98
Vermiculite	(K)	$K_{0.86}Mg_3Si_{3.14}Al_{0.86}O_{10}(OH)_2$	-6173.41	310.21	12.15	350.19	147.56
	(Na)	$Na_{0.86}Mg_3Si_{3.14}Al_{0.86}O_{10}(OH)_2$	-6143.26	322.45	12.15	348.34	145.71
	(Ca)	$Ca_{0.43}Mg_3Si_{3.14}Al_{0.86}O_{10}(OH)_2$	-6148.06	299.63	12.15	336.40	149.80
	(Mg)	$Mg_{0.43}Mg_3Si_{3.14}Al_{0.86}O_{10}(OH)_2$	-6113.11	301.31	12.15	333.46	139.69
Berthierine(FeIII)		$(Fe^{+2}{}_{2.34}Fe^{+3}{}_{0.33}Al_{0.33})(Si_{1.34}Al_{0.66})O_5(OH)_4$	-3458.03	251.74	36.23[(a)]	297.41	103.27
Berthierine(FeII)		$(Fe^{+2}{}_2Al)(SiAl)O_5(OH)_4$	-3770.46	226.31	26.76[(a)]	283.50	103.86
Cronstedtite		$(Fe^{+2}{}_2Fe^{+3})(SiFe^{+3})O_5(OH)_4$	-2914.55	256.60	56.56[(a)]	257.02	76.80
Glauconite		$K_{0.75}(Mg_{0.25}Fe^{+2}{}_{0.25}Fe^{+3}{}_{1.25}Al_{0.25})(Al_{0.25}Si_{3.75})O_{10}(OH)_2$	-5151.13	314.92	51.66	344.54	139.76

(a) Configurational entropy is not considered here, following Bertoldi and others (2007) and Blanc and others (2014)

lonite. This situation is not surprising compared with the results obtained by Roy and Romo (1957), Whitney (1983) and Mosser-Ruck and others (2010), where clinochlore and vermiculite are rather restricted to high temperature domains. In figures 12A and 12B, illite (Al) is found to be more stable than muscovite. We could test that considering an ordered muscovite rather than a disordered one, as in the present

TABLE 15

Thermodynamic properties of zeolites

Mineral	Formula	LogK (25 °C)	ΔH_f^0 kJ.mol^{-1}	Δ kJ.mol^{-1}	S^0 J.mol^{-1}.K^{-1}	Δ J.mol^{-1}.K^{-1}	V° cm^3.mol^{-1}	Cp (25 °C) J.mol^{-1}.K^{-1}
Analcime	$Na_{0.99}Al_{0.99}Si_{2.01}O_6:H_2O$	*6.64*	-3308.00[a]	3.3	231.08[a]	0.23	97.09[a]	212.38[b]
Phillipsite(K)	$KAlSi_3O_8:3H_2O$	0.04[c]	*-4841.86*		390.57[d]	1.20	148.97[e]	351.41
Phillipsite(Na)	$NaAlSi_3O_8:3H_2O$	1.45[c]	*-4811.66*		382.53[d]	1.20	149.69[e]	330.96
Phillipsite(Ca)	$Ca_{0.5}AlSi_3O_8:3H_2O$	2.32[c]	*-4824.02*		342.38[d]	1.20	151.15[e]	321.86
Natrolite	$Na_2(Al_2Si_3)O_{10}:2H_2O$	*19.31*	-5718.60[f]	5.5	359.73[f]	0.72	169.20[g]	359.23[f]
Scolecite	$CaAl_2Si_3O_{10}:3H_2O$	*16.63*	-6049.00[f]	5.5	367.42[f]	0.73	172.30[g]	382.81[f]
Stilbite	$NaCa_2(Al_5Si_{13})O_{36}:16H_2O$	*3.74*	-22579.71[h]		1622.56[h]		664.70[h]	1697.03[h]
Stellerite	$Ca_2Al_4Si_{14}O_{36}:14H_2O$	*6.90*	-21656.24[h]		1604.73[h]		666.50[h]	1573.96[h]
Mordenite(Ca)	$Ca_{0.515}Al_{1.03}Si_{4.97}O_{12}:3.1H_2O$	-2.92[i]	*-6662.19*		493.57[j]		209.80[j]	443.11[g]
Mordenite(J)	$Ca_{0.289}Na_{0.362}Al_{0.94}Si_{5.06}O_{12}:3.468H_2O$	*-4.18*	-6738.44[k]	4.5	486.54[k]	0.97	212.40[k]	484.45[k]
Clinoptilolite(Ca)	$Ca_{0.55}(Si_{4.9}Al_{1.1})O_{12}:3.9H_2O$	-2.35[i]	*-6923.33*		498.99[i]		209.66[e]	481.02[j]
Clinoptilolite(Na)	$Na_{1.1}(Si_{4.9}Al_{1.1})O_{12}:3.5H_2O$	-0.09[l]	*-6782.36*		502.72[l]		214.78[e]	470.38[j]
Clinoptilolite(K)	$K_{1.1}(Si_{4.9}Al_{1.1})O_{12}:2.7H_2O$	-1.23[l]	*-6568.41*		507.66[l]		210.73[e]	454.31[j]
Merlinoite(Na)	$Na_{1.04}Al_{1.04}Si_{1.96}O_6:2.27H_2O$	*10.54*	-3681.43[m]		283.43[m]		114.04[m]	305.68[m]
Merlinoite(K)	$K_{1.04}Al_{1.04}Si_{1.96}O_6:1.69H_2O$	*11.59*	-3537.60[m]		270.48[m]		112.91[m]	249.65[m]
ZeoliteCaP	$Ca_2Al_4Si_4O_{16}:9H_2O$	45.15[n]	-11129.11[n]		*975.40*		305.70[e]	872.11[j]
Wairakite	$CaAl_2Si_4O_{12}:2H_2O$	*14.42*	-6646.70[p]	6.3	400.70[p]		193.56[e]	401.04[q]
Laumontite	$CaAl_2Si_4O_{12}:4H_2O$	*11.66*	-7251.00[p]	5.6	483.80[r]	2.10	207.53[e]	542.23[j]
Heulandite(Ca)	$Ca_{1.07}Al_{2.14}Si_{6.86}O_{18}:6.17H_2O$	2.46[n]	-10667.20[s]	8.6	*700.94*		322.06[e]	719.05[j]
Heulandite(Na)	$Na_{2.14}Al_{2.14}Si_{6.86}O_{18}:6.17H_2O$	2.80[n]	-10612.85[s]	8.6	*838.29*		325.00[e]	719.05[j]
Gismondine	$Ca_2Al_4Si_4O_{16}:9H_2O$	*38.96*	-11179.80[o]		742.24[j]		315.07[e]	869.26[j]
Chabazite	$CaAl_2Si_4O_{12}:6H_2O$	*11.51*	-7826.44[t]		614.00[u]		251.16[e]	681.19[j]

In italics: internally recalculated values; (a) Neuhoff and others (2004); (b) Johnson and others (1982); (c) Calculated by combining data from Hess (1966) and Shibue (1981); (d) Extracted from Hemingway and Robie (1984); (e) from Coombs and others (1997) density value; (f) Johnson and others (1983); (g) Robie and Hemingway (1995); (i) After Benning and others (2000); (j) Estimated using Vieillard's (2010) method; (k) Johnson and others (1992); (l) After Wilkin and Barnes (1998); (m) After Donahoe and others (1990); (n) Blanc and others (2010); (o) Estimated using Chermak and Rimstidt's (1989) method; (p) Kiseleva and others (1996); (q) Neuhoff and Wang (2007); (r) Paukov and Fursenko (1998); (s) After Kiseleva and others (2001); (t) After Shim and others (1999); (u) After Belitskii and others (1982).

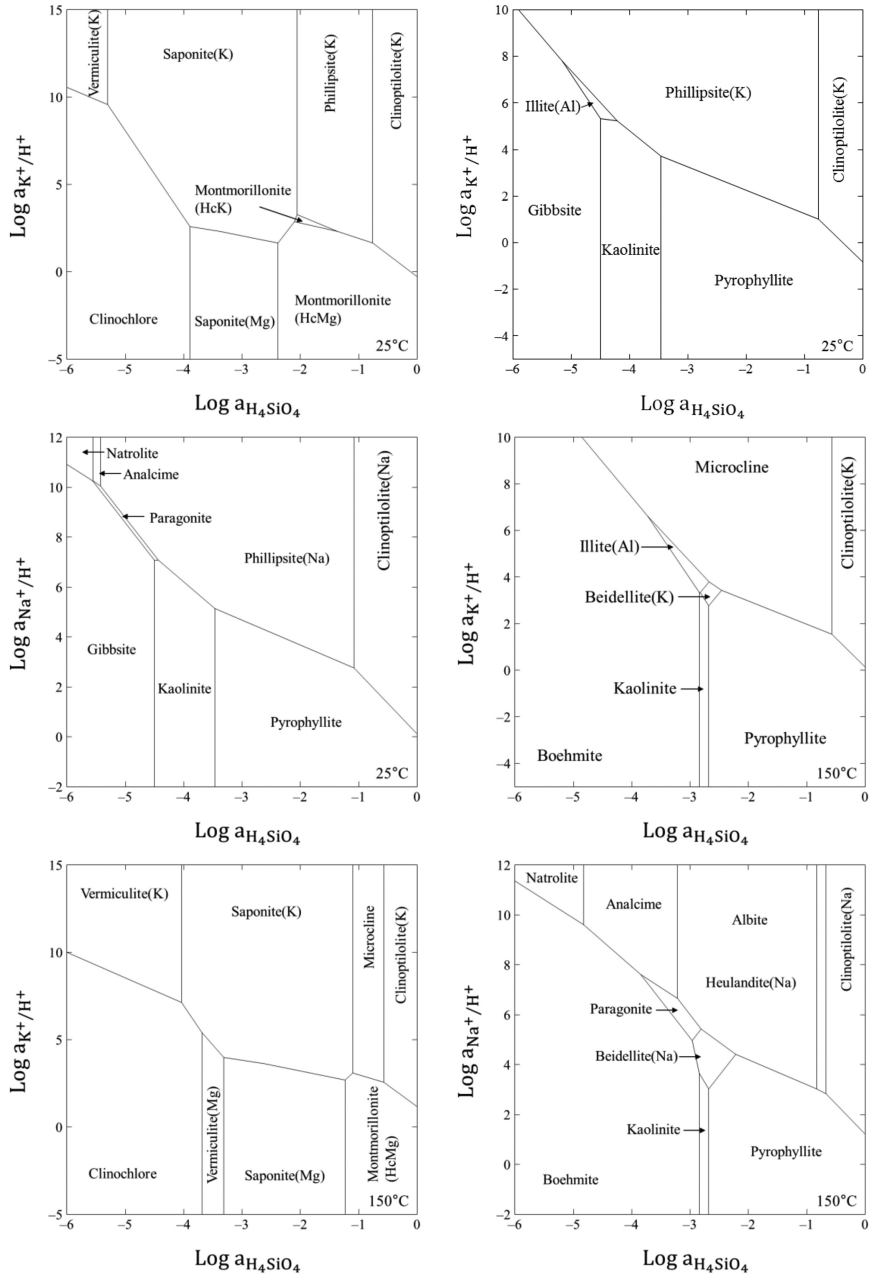

Fig. 12. Activity diagrams in the SiO_2-Al_2O_3-MgO-K_2O-Na_2O-H_2O system. (A) Sub-system SiO_2-Al_2O_3-K_2O-H_2O at 25 °C; (B) Sub-system SiO_2-Al_2O_3- K_2O-H_2O at 150 °C; (C) Sub-system SiO_2-Al_2O_3-MgO-K_2O-H_2O at 25 °C, equilibrium with talc; (D) Sub-system SiO_2-Al_2O_3-MgO-K_2O-H_2O at 150 °C equilibrium with talc; (E) Sub-system SiO_2-Al_2O_3- Na_2O-H_2O at 25 °C; (F) Sub-system SiO_2-Al_2O_3- Na_2O-H_2O at 150 °C. Equilibrium constants calculated using thermodynamic properties from table 1, table 14 and table 15, for the corresponding minerals.

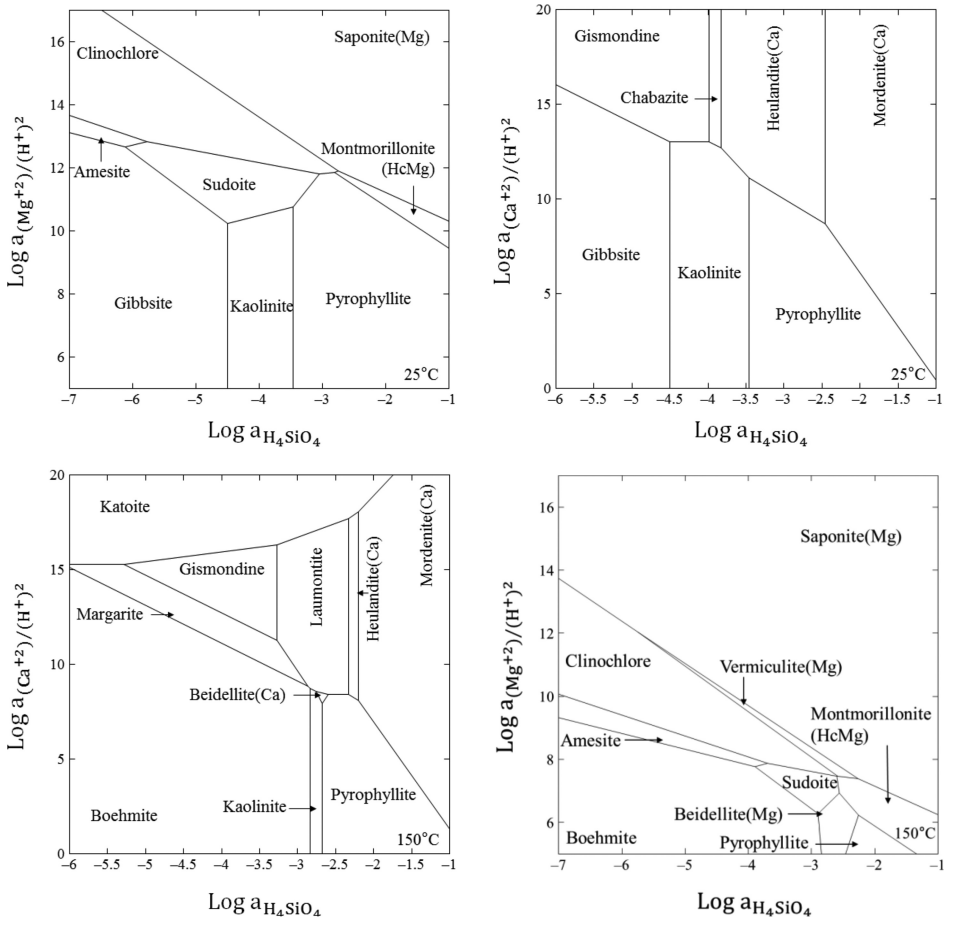

Fig. 13. Activity diagrams in the SiO_2-Al_2O_3-MgO-CaO-H_2O system. (A) Sub-system SiO_2-Al_2O_3-CaO-H_2O at 25 °C; (B) Sub-system SiO_2-Al_2O_3- CaO-H_2O at 150 °C; (C) Sub-system SiO_2-Al_2O_3-MgO-H_2O at 25 °C; (D) Sub-system SiO_2-Al_2O_3-MgO-H_2O at 150 °C. Equilibrium constants calculated using thermodynamic properties from table 1, table 14 and table 15, for the corresponding minerals.

selection, was reversing this tendency. This indicates small affinities for the mineral transformation from illite to muscovite, with respect to the uncertainties related to the present estimates, which prevent us from discussing this point in greater depth.

Figures 13A to 13D display quite similar tendencies for the chemical system SiO_2-Al_2O_3-MgO-CaO-H_2O, at 25 °C and 150 °C. Figures 13A and 13B in particular allow the discussion on zeolites to be completed. Indeed, the comparison between the 25 °C and 150 °C figures indicates a transition between low temperature phases such as gismondine, chabazite or phillipsite, to a set of minerals stable at higher temperatures such as laumontite, for instance, or microcline and albite. Such modifications correspond to an evolution of the zeolite paragenesis with temperature, as reported by Fridriksson and others (2001) or Giret and others (1992). Figures 13C and 13D are dominated by the 14 Å phases. This is because aluminium is present in the system. Otherwise, 7 Å phases would appear instead, as reported in figure 14D for the iron chemical sub-system.

For the SiO_2-Al_2O_3-MgO-FeO- Fe_2O_3-Na_2O-H_2O system, figures 14A to 14D provide the stability domains at 25 °C, especially for the iron-bearing phases. This

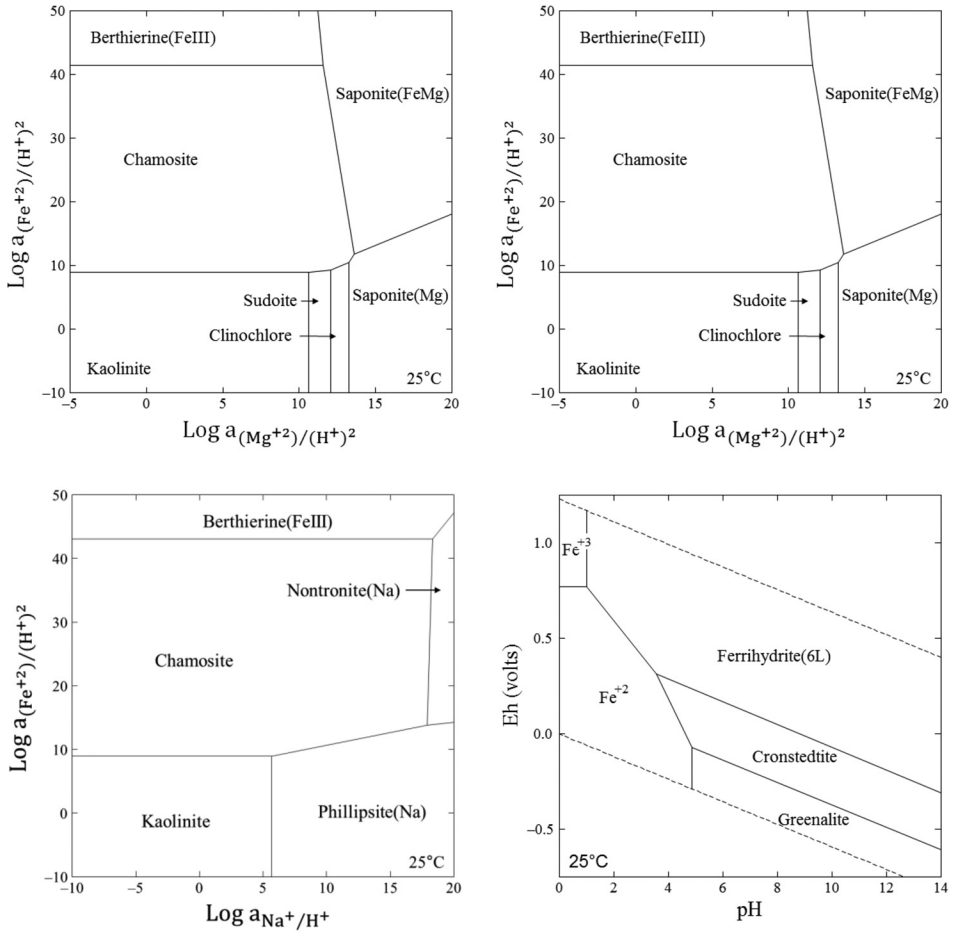

Fig. 14. Activity diagrams in the SiO_2-Al_2O_3-MgO-FeO-Fe_2O_3-Na_2O-H_2O system. (A) Sub-system SiO_2-Al_2O_3-FeO-Fe_2O_3-Na_2O-H_2O at 25 °C, Log(Na+/H+) = 5, equilibrium with quartz; (B) Sub-system SiO_2-Al_2O_3-FeO-Fe_2O_3-Na_2O-H_2O at 25 °C, equilibrium with quartz, $Logf_{O2,g}$ = -70; (C) Sub-system SiO_2-Al_2O_3-MgO-FeO-Fe_2O_3- H_2O at 25 °C, equilibrium with quartz, $Logf_{O2,g}$ = -70; (D) Sub-system SiO_2-FeO-Fe_2O_3-H_2O at 150 °C, equilibrium with quartz, no iron oxides/hydroxides but ferrihydrite.

chemical model has been the subject of several important studies in the past. Among the latter, the studies from Wilson and others (2006) and Mosser-Ruck and others (2010) give indications that can be compared with the present results. In table 14, berthierine(FeII) has the same composition as the phase used by Wilson and others (2006). In our case, Chamosite appears instead, since berthierine (FeII) is less stable by 168 kJ/mol, in our case. In fact, berthierine does appear but in the highest part of the diagram and extends towards higher $Logf_{O2,g}$, which results from its Fe^{+3} content. Apart from the position of the stability field of berthierine, figures 14A and 14B are quite similar to Wilson and others (2006) Figures 4A and 4B at 25 °C. Such similarity is less evident in figure 14C (equivalent to fig. 8A) at 25 °C in Wilson and others (2006) since amesite from our selection is less stable by 190 kJ/mol per $O_{10}(OH)_8$. Finally, figure 14D indicates that, at equilibrium with quartz, cronstedtite appears at equilibrium with ferrihydrite, whereas the presence of the other iron oxides/hydroxides

prevents this. Greenalite remains stable in the lowest Eh domains, even when hematite (the most stable oxide) is considered in the system.

CONCLUSIONS

In order to provide a database for the thermodynamic properties of clay minerals, the present work proposes a set of estimation models. The developments concern the estimates for the enthalpies, the entropies, the heat capacities and the molar volumes. Two different prediction models have been developed, one based on the electronegativity scale for the enthalpy alone and a second polyhedral decomposition model, for all other properties. For the latter, the electronegativity relation has been proposed in order to provide it with an extrapolation capacity for chemical elements not included into the parameterization set of minerals. Both models use the same set of minerals for deriving their internal constants and for verification. This ensures an overall consistency between both approaches. In addition, the data, selected from a literature review, can represent the first block of thermodynamic data for building up a consistent database for phyllosilicates. The consistency of both types of models could be tested by verifying the Gibbs energy function that combines both enthalpy and entropy terms. The models result in an overall improvement of the estimates with respect to previous models. Finally, they have been used to calculate the thermodynamic functions of a large set of clay minerals, providing a consistent thermodynamic database that can be used for geochemical calculations that involve such phases. The database is tested by drawing a predominance diagram in selected chemical subsystems of interest. Since this work does not include the hydration contribution to the overall Gibbs energy (Vidal and Dubacq, 2009; Vieillard and others, 2011), phase relations may still be modified, especially for hydrated clay minerals. Future developments may need to pay attention to this additional contribution.

ACKNOWLEDGMENTS

Financial support from the French National Radioactive Waste Management Agency (ANDRA) and from the French Geological Survey (BRGM) is gratefully acknowledged. The authors would like to thank D. Rimstidt for his kind support and an anonymous reviewer for his critical and constructive remarks.

APPENDIX 1

DETAILED SELECTION FOR THERMODYNAMIC PROPERTIES OF PHYLLOSILICATES

This appendix describes the selection of phyllosilicate thermodynamic data from the literature. It includes a specific section for the phases that have been the subject of a single study, for which the discussion is limited. A comparison is provided, with respect to the results obtained after a recent global optimization work by Tutolo and others (2014). The values eventually selected are fully reported in table 1. For kaolinite, the selection is already discussed by Blanc and others (2013).

Datasets Built from Direct Measurements

Muscovite and pyrophyllite.—The entropies of muscovite and pyrophyllite were measured by Robie and others (1976), whose results were adopted by Robie and Hemingway (1995) and Haselton and others (1995) as reference values; we also selected these values. The heat capacity comes from the work from Krupka and others (1979), knowing that this represents the only direct measurement of S^0 and Cp(T) for the two phases. For the enthalpy of formation of muscovite, the value of –5.946.20 kJ/mol measured by Barany (1964) was modified to –5.976.74 kJ/mol by Hemingway and Robie (1977) and Berman (1988) because of a 11.3 kJ/mol correction on the enthalpy of formation for gibbsite. This value would characterize a phase where Al and Si are partly ordered in the tetrahedral layer (Haselton and others, 1995). Robie and Hemingway (1995) provide the thermodynamic properties for ordered and disordered muscovite, but they refer to a document that does not completely explain the process for calculating the enthalpy of formation and its origin remains difficult to assess. The values found in the literature mostly come from the exploitation of high temperature (between 510 and 802 °C) and high pressure (from 1 – 6 kbars) reaction data (Chatterjee and Johannes, 1974; Haselton and others, 1995). Among these, we selected the value of –5974.80 kJ/mol, given by Haselton

and others (1995), after equilibria experiments. It comes from recent, traceable experiments focused on muscovite, with detailed chemical and mineralogical analyses and an extensive discussion on the influence of disorder in the tetrahedral layers. The work by Haselton and others (1995) would, moreover, relate to a relatively disordered 1M phase, which appears better adapted to the construction of a prediction model for clay minerals. The polytype difference could explain the 10 kJ/mol discrepancy observed with the value provided by Holland and Powell (1998) for a 2M1 muscovite sample. Tutolo and others (2014) obtained −5982.70 J/mol and 292.00 J/mol.K for the enthalpy and the entropy, respectively, which could apply rather to the 2M1 polytype. Few studies have been carried out so far concerning pyrophyllite formation enthalpy. Using the result of experiments carried out at high pressure and high temperature, Robie and Hemingway (1995), Holland and Powell (1998), Gottschalk (1997) and Chatterjee and others (1998) obtained an enthalpy of formation that is within ± 0.5kJ/mol. We adopted the value provided by Robie and Hemingway (1995), that is –5.640.00±1.50 kJ/mol. The value refined by Tutolo and others (2014), −5638.78 kJ/mol, agrees with this selection, given the uncertainty.

Phlogopite.—The enthalpy of formation for phlogopite measured by Circone and Navrotsky (1992) is the only available direct measurement, as opposed to the values given by Robie and Hemingway (1995), which are estimates. The entropy of phlogopite given by Robie and Hemingway (1984) and Hemingway (1991) is from the most recent direct measurement. With respect to the case of muscovite, for example, the discussion is more limited given the few direct measurements available in the literaure.

Paragonite.—The paragonite case is very similar to the previous one. The enthalpy of formation measured by Roux and Hovis (1996) is the only direct measurement available, as opposed to the values given by Robie and Hemingway (1995), which are estimates. The refinement performed by Tutolo and others (2014) results in -5956.34 kJ/mol and 276.02 J/mol.K for the enthalpy and the entropy, respectively, which are closer to the values reported by Robie and Hemingway (1995) for an ordered phase (-5949.30 kJ/mol), whether Roux and Hovis (1996) obtained -5937.50± 3.0 which is closer to the value reported by Robie and Hemingway (1995) for the disordered phase (-5933.00 kJ/mol). The entropy reported by Robie and Hemingway (1984) is currently the most recent direct measurement available.

Talc.—The enthalpy of formation of talc was measured and discussed by Kahl and Maresch (2001). These authors show that all the measurements carried out over the past 20 years are, within the uncertainty, consistent among themselves as long as a consistent database is used to calculate the thermodynamic cycles. The directly measured values were all acquired from high temperature dissolution reactions, with lead borate as solvent. In that case, extracting the enthalpy of formation at 25 °C requires that the Cp(T) and ΔH°_f of the minerals used in each thermodynamic cycle are known. Kahl and Maresch (2001) used the Holland and Powell (1998) database, which is self-consistent. Moreover, the value obtained by these authors comes from three different thermodynamic cycles including a sensitivity analysis of the critical volatile component H_2O. For the above reasons, we have used the value proposed by Kahl and Maresch (2001), −5.892.10 kJ/mol. For the entropy and heat capacity, we retained the values measured by Robie and Stout (1963) and Krupka and others (1979), which are the only direct measurements available for a composition close to the ideal formula.

Natural 2:1 clay minerals.—Recently, full sets of thermodynamic data have been measured for natural 2:1 clay minerals. These include:

— Illite/Smectite ISCz-1 (Gailhanou, ms, 2005),
— Illite IMt-2, Smectite MX-80, Beidellite SBId-1 (Gailhanou and others, 2012)
— Nontronite Nau-1, Saponite SapCa-1, Vermiculite Santa Olalla (SO) (Gailhanou and others, 2013).

Most of these are retained to parameterize the models. Because verification also has to rely on some accurately measured data, Beidellite SBId-1, Saponite SapCa-1 and Illite/Smectite ISCz-1 have been used for this purpose in the present work.

Chlorite (ripidolite) and berthierine.—The determination of the full set of thermodynamic parameters has been carried out recently by Blanc and others (2014) on a CCa-2 chlorite sample and a berthierine sample from Illinois (USA). The values have been directly retained for the present work, since no other study has proposed a consistent set of directly measured thermodynamic properties for these phases.

Sepiolite.—Sepiolite properties are obtained by Stoessell (1988) from a series of solubility experiments performed at different temperatures. They are compared by the author to the assessment given by previous authors. Stoessel's (1988) study provides the only data set of directly measured thermodynamic properties available for sepiolite.

Datasets Built from Indirect Measurements

In this category are gathered the minerals for which all the properties are derived from equilibria realized at high temperature and pressure. The properties extrapolated to 25 °C thus depend on the Cp(T) functions used by the authors and on the thermodynamic parameters of the other reactive species and products of the reaction.

Annite.—In spite of the lack of precise detail, it seems that the thermodynamic functions S^0 and Cp(T) given by Robie and Hemingway (1995) were estimated from measurements carried out on a natural phase by Hemingway and Robie (1990). This phase actually contained 1.0 F and 0.8 Al in the octahedral sheet per $O_{10}(OH)_2$. Robie and Hemingway (1995) have corrected the measurements for a purely ferrous mineral, devoid of fluorine. Unfortunately, the correction method is not indicated. Moreover, Robie and Hemingway (1995) selected the enthalpy of formation published by Holland and Powell (1990), which was based on a single series of equilibrium experiments. Finally, the entropy and enthalpy of formation are selected from the experimental work of Dachs and Benisek (1995). This choice was made for the sake of consistency and because the authors have carried out reversed equilibrium experiments and have conducted a sensitivity analysis on their results, based on different databases.

Margarite.—The values published by Robie and Hemingway (1995) are very close to those obtained by Holland and Powell (1998), with only 1 kJ/mol difference for the enthalpy of formation and 3 J/mol.K for the entropy. Robie and Hemingway's (1995) selection was preferred, for the sake of consistency with the rest of this work. For the Cp(T) function, we selected the values of Robinson and others (1982) rather than those of Robie and Hemingway (1995), since the calculation method is reported by the authors.

Minnesotaite and greenalite.—Evans and Guggenheim (1988) have proposed the properties of minnesotaite, with the following composition $Fe_3Si_4O_{9.6}(OH)_{2.8}$. The assessment was made after a compilation of experimental studies performed at high temperature and pressure and field observations. Using their own experiments at high temperature and pressure, Rasmussen and others (1998) obtained the properties of greenalite, using the data of Evans and Guggenheim (1988) for the properties of minnesotaite. Unfortunately, the latter do not provide any explanation concerning the choice of thermodynamic properties for minnesotaite. On the other hand, Miyano and Klein (1983) have also assessed the properties of minnesotaite and greenalite. Because the details of the assessment process are fully described by these authors, we have chosen to retain the values of the properties published by Miyano and Klein (1983).

Chrysotile and lizardite.—Chrysotile and lizardite properties have been synthesized and reviewed in a recent review paper by Evans (2004). Taking advantage of previous studies and direct measurements for chrysotile, the author concluded in the metastability of chrysotile and deduced the properties of lizardite with respect to those compiled for chrysotile. The properties reviewed and selected by Evans (2004) are retained here.

Antigorite.—Antigorite properties are derived from the database of Holland and Powell (1998). Indeed, they are the only authors providing a full dataset of thermodynamic properties and who actually consider antigorite with a chemical formula that corresponds to that of the natural mineral. For Robie and Hemingway (1995), antigorite is confused with chrysotile.

Chlorites.—For chlorites, the properties published by Vidal and others (2005) for five end-members (clinochlore, chamosite, amesite, Fe-amesite and sudoite) resulted from a long series of previously published experimental studies. Few papers report direct measurements. These are limited to the entropy and the Cp(T) functions (Hemingway and others, 1984; Bertoldi and others, 2007). Because the Cp(T) function published by Saccocia and Seyfried (1993) starts at 50K only, it has been discarded from the present discussion. Hemingway and others (1984) and Bertoldi and others (2007) values are selected here but for the set of verification minerals since, for parameterization, we favor complete thermodynamic datasets for the sake of consistency. Similarly, since the experimental dataset used by Holland and Powell (1998) to retrieve the properties of Mg-chlorite and Fe-sudoite, both phases were selected for verification only.

Celadonite, Fe-celadonite, Na-phlogopite, Eastonite and Siderophyllite.—The thermodynamic properties are selected after Coggon and Holland (2002) and Holland and Powell (1998). The retrieval method is quite similar to the previous one, in that a solid solution model is used in order to derive the properties of these end-members. However, the experimental dataset is much more reduced than the one used by Vidal and others (2005) for chlorite end-members.

Incomplete Datasets

Some incomplete datasets have also been included in the selection for verification purposes. These include the datasets from:

— Robie and others (1976) for illite;
— Bertoldi and others (2005) for berthierine;
— Bertoldi, Dachs and Appel (2007) for chlorites;
— Hemingway and others (1984) for chlorites;
— Ogorodova and others (2009) for a vermiculite.

In fact, a formation enthalpy was provided by Bertoldi and others (2005), together with the measured entropy. Unfortunately, it was based on a berthierine/chlorite transition reaction that was hypothesized after field observations. This value was not retained for the present work.

APPENDIX 2

SELECTION FOR ZEOLITE MINERALS

Among the minerals involved in the context of cement/clay interactions, zeolites are a group of important phases, which represent a transition between cementitious material and the clayey barrier (Gaucher and Blanc, 2006). This Appendix reports a selection of thermodynamic properties, based on a literature review, for zeolite minerals. When required, the thermodynamic datasets have been completed by using estimation models, as described below.

Selection Principles

The selection of thermodynamic properties is focused on the collection of direct and traceable measurements, according to the following guidelines:

— To avoid fitting of the LogK(T) functions, as well as averaging equilibrium constants. The aim is to avoid producing new and perhaps confusing data.

— When possible, to calculate LogK(T) functions by using calorimetric data (and/or estimates) and to compare them with the results of solution equilibria experiments in order to perform an independent verification. The whole process could be achieved only for analcime.

— Thermodynamic calculations are realized consistently, using the same secondary or auxiliary properties.

— The selection is finally verified by drawing activity diagrams involving the minerals of interest in the chemical sub-systems of concern.

Additional details for selection are given in Blanc and others (2015). As can be seen in table 15, most of the Cp(25 °C) had to be estimated since very few direct measurements were available. Moreover, for chabazite, heulandite, laumontite and wairakite, the phase transition temperature could be checked with respect to experimental results from Liou (1971), Zeng and Liou (1982) and Cho and others (1987), by calculating their LogK(T) function.

Johnson and Others (1992) Corrections

In a series of papers, (Johnson and others, 1982, 1983, 1985, 1991 and 1992; Howell and others, 1990) measured a complete set of thermodynamic data for analcime, natrolite, mesolite, scolecite, heulandite, clinoptilolite and mordenite. These sets of consistent and direct measurements represent the core of the present selection. However, in a final paper, Johnson and others (1992) proposed correcting all their previous enthalpy measurements by –3.51 kJ/mol per Si atom, based on a re-evaluation of silicalite formation enthalpy. Integrating this modification leads to the disappearance of the analcime stability field in figure 12F. Following Neuhoff and others (2004), we have preferred not to retain this correction for analcime and the other phases measured by Johnson and co-workers.

Predictive Models

In order to complete the thermodynamic property sets we had to rely on estimation models in some cases. This was limited to the heat capacity at 25 °C and to entropy (2 minerals, see table 15). Estimates were made using the method recently published by Vieillard (2010). The comparison with calorimetric measurements displayed an overall improvement of 5 percent for the entropy and 10 percent for the specific heat with respect to the previous estimation methods. The latter were primarily based on the polyhedral approach. An improvement proposed by Vieillard (2010) can be made by (1) using the thermodynamic properties of silica polymorphs, whose crystal structure is close to that of zeolite, and (2) determining specifically the thermodynamic parameters of the zeolitic water. Thus Vieillard (2010) has proposed new sets of entropies and Maier-Kelley coefficients a, b and c for the heat capacity function, for the various oxides which compose zeolites. With the new sets of values, prediction errors decrease to less than 3 percent and 4 percent for the entropy and the specific heat, respectively.

Selected Properties by Mineral Type

The thermodynamic constants finally selected for zeolites are reported in table 15. A brief explanation is given next for each phase and additional details are given in Blanc and others (2015):

Analcime.—Analcime properties are derived from the very complete review by Neuhoff and others (2004) and verified against solubility data from Murphy and others (1996) and Wilkin and Barnes (1998).

Phillipsite.—Log K (25 °C) is derived from a calculation process from Hess (1966) that is based on equilibrium with microcline in a saline environment. The proposed equilibrium could not be checked. Entropy and heat capacity are derived from Hemingway and Robie (1984) measurements.

Scolecite and natrolite.—For both phases, a complete set of measurements is provided by Johnson and others (1983).

Stilbite and stellerite.—The thermodynamic function has been reviewed by Fridriksson and others (2001).

Mordenite.—A complete thermodynamic dataset has been measured by Johnson and others (1992) [mordenite (J) in table 15]. However the LogK(T) function calculated from these data is not compatible with Wilkin and Barnes (1998) and Benning and others (2000) solution experiment results [Mordenite(Ca) in table 15]. Consistency is regained by removing the correction applied by Johnson and others (1992) to the formation enthalpy.

Clinoptilolite.—A full set of thermodynamic parameters is given by Johnson and others (1991). Unfortunately, the natural sample chosen contains Ba and Sr, which poses problems for future modeling. Instead, we have extracted thermodynamic functions from Benning and others (2000) and Wilkin and Barnes (1998) solution experiments, coupled with Yang and others (2001) experimental determination of the formation enthalpy.

Merlinoite.—For this phase, the selection is based on a single experimental work by Donahoe and others (1990).

Zeolite CaP.——Because of a lack of experimental data, LogK(298) is inferred from phase relation in cementitious systems by Blanc and others (2010). It may replace gismondine as a synthetic analogue, for cementitious systems especially.

Wairakite.—The thermodynamic functions are taken from calorimetric measurements by Kiseleva and others (1996).

Laumontite.—The selection is based on the direct measurements performed by Kiseleva and others (1996) and Paukov and Fursenko (1998).

Heulandite.—The selection is based on the experimental work of Drebushchak and others (2000) and Kiseleva and others (2001). To derive the properties of pure end-members, exchange properties are extracted from the work of Fridriksson and others (2001) and (2004).

Gismondine.—The selection is rather uncertain for this phase. Both enthalpy and entropy are estimated and the verification performed by Blanc and others (2015) is very limited.

Chabazite.—The thermodynamic functions are directly measured by Shim and others (1999) and Belitskii and others (1982), for the formation enthalpy and the entropy, respectively, on a mineral displaying the same composition in both studies.

Finally, the consistency of phase relation is tested by drawing the activity diagrams in figures 12 to 14. Problems remain concerning specifically phillipsite and gismondine, due to a lack of experimental data in the literature.

— Gismondine, which has to be discarded from the selection.

— The phillipsite(Na) stability domain is also a matter of discussion in that it partially overlaps that of analcime.

— Experimental data are lacking in order to address more accurately the stability domains of phillipsite, chabazite and gismondine.

In addition, for verification we used data derived either from experiments or from field investigations. This poses some difficulty since it involves many parameters to consider.

REFERENCES

Aagaard, P., and Helgeson, H. C., 1983, Activity/composition relations among silicates and aqueous solutions: II. Chemical and thermodynamic consequences of ideal mixing of atoms on homological sites in montmorillonites, illites and mixed layer clays: Clays and Clay Minerals, v. 31, n. 3, p. 207–217, http://dx.doi.org/10.1346/CCMN.1983.0310306

Aagaard, P., and Jahren, J. S., 1992, Diagenetic illite-Chlorite assemblages in arenites. II. Thermodynamic relations: Clays and Clay Minerals, v. 40, n. 5, p. 547–554, http://dx.doi.org/10.1346/CCMN.1992.0400508

Aja, S. U., Rosenberg, P. E., and Kittrick, J. A., 1991, Illite equilibria in solutions: I. Phase relationships in the system K_2O-Al_2O_3-SiO_2-H_2O between 25 and 250 °C: Geochimica et Cosmochimica Acta, v. 55, n. 5, p. 1353–1364, http://dx.doi.org/10.1016/0016-7037(91)90313-T

Barany, R., 1964, Heat and Free Energy of Formation of Muscovite: U.S. Bureau of Mines Report Investigation, 6 p.

Belitskii, I. A., Gabuda, S. P., and Drebushchak, V. A., 1982, The heat capacity of Chabazite at 5-316K, the entropy and the enthalpy under standard conditions: Geokhimiya, v. 5, p. 756–764.

Benning, L. G., Wilkin, R. T., and Barnes, H. L., 2000, Solubility and stability of zeolites in aqueous solution: II. Calcic clinoptilolite and mordenite: American Mineralogist, v. 85, n. 3–4, p. 495–508.

Berman, R. G., 1988, Internally consistent thermodynamic data for minerals in the system Na_2O-K_2O-CaO-MgO-FeO-Fe_2O_3-Al_2O_3-SiO_2-TiO_2-H_2O-CO_2: Journal of Petrology, v. 29, n. 2, p. 445–522, http://dx.doi.org/10.1093/petrology/29.2.445

Berman, R. G., and Brown, T. H., 1985, Heat capacity of minerals in the system Na_2O-K_2O-CaO-MgO-FeO-Fe_2O_3-Al_2O_3-SiO_2-TiO_2-H_2O-CO_2, representation, estimation and high temperature extrapolation: Contributions to Mineralogy and Petrology, v. 89, n. 2–3, p. 168–183, http://dx.doi.org/10.1007/BF00379451

Bertoldi, C., Dachs, E., Cemic, L., Theye, T., Wirth, R., and Groger, W., 2005, The heat capacity of the serpentine subgroup mineral Berthierine ($Fe_{2.5}Al_{0.5}$)[$Si_{1.5}Al_{0.5}O_5$]$(OH)_4$: Clays and Clay Minerals, v. 53, n. 4, p. 380–388, http://dx.doi.org/10.1346/CCMN.2005.0530406

Bertoldi, C., Dachs, E., and Appel, P., 2007, Heat-pulse calorimetry measurements on natural chlorite-group minerals: American Mineralogist, v. 92, p. 553–559, http://dx.doi.org/10.2138/am.2007.2247

Blanc, P., Bourbon, X., Lassin, A., and Gaucher, E. C., 2010, Chemical model for cement-based materials: Thermodynamic data assessment for phases other than C–S–H: Cement and Concrete Research, v. 40, n. 9, p. 1360–1374, http://dx.doi.org/10.1016/j.cemconres.2010.04.003

Blanc, P., Lassin, A., Piantone, P., Azaroual, M., Jacquemet, N., Fabbri, A., and Gaucher, E. C., 2012, Thermoddem: A geochemical database focused on low temperature water/rock interactions and waste materials: Applied Geochemistry, v. 27, n. 10, p. 2107–2116. http://dx.doi.org/10.1016/j.apgeochem.2012.06.002

Blanc, P., Vieillard, P., Gailhanou, H., and Gaboreau, S., 2013, Thermodynamics of Clay Minerals, *in* Bergaya, F., and Lagaly, G., editors, Handbook of Clay Science: Developments in Clay Science, v. 5, Chapter 6, p. 173–210, http://dx.doi.org/10.1016/b978-0-08-098258-8.00006-7

Blanc, P., Gailhanou, H., Rogez, J., Mikaelian, G., Kawaji, H., Warmont, F., Gaboreau, S., Grangeon, S., Grenèche, J.-M., Vieillared, P., Fialips, C. I., Giffaut, E., Gaucher, E. C., and Claret, F., 2014, Thermodynamic properties of chlorite and berthierine derived from calorimetric measurements: Physics and Chemistry of Minerals, v. 41, n. 8, p. 603–615, http://dx.doi.org/10.1007/s00269-014-0683-z

Blanc, P., Vieillard, P., Gailhanou, H., Gaboreau, S., Marty, N., Claret, F., Madé, B., and Giffaut, E., 2015, ThermoChimie database developments in the framework of cement/clay interactions: Applied Geochemistry, Geochemical Speciation Codes and Databases, v. 55, p. 95–107, http://dx.doi.org/10.1016/j.apgeochem.2014.12.006

Bryndzia, L. T., and Scott, S. D., 1987, The composition of chlorite as a function of sulfur and oxygen fugacity. An experimental study: American Journal of Science, v. 287, n 1, p. 50–76, http://dx.doi.org/10.2475/ajs.287.1.50

Chase, M. W., Jr., 1998, NIST-JANAF thermochemical tables. Part I, Part II: Washington, D. C., American Chemical Society, American Institute of Physics for the National Institute of Standards and Technology, Monograph 9, 1963 p.

Chatterjee, N. D., and Flux, S., 1986, Thermodynamic Mixing Properties of Muscovite-Paragonite Crystalline Solutions at High Temperatures and Pressures, and their Geological Applications: Journal of Petrology, v. 17, n. 3, p. 677–693, http://dx.doi.org/10.1093/petrology/27.3.677

Chatterjee, N. D., and Johannes, W., 1974, Thermal stability and standard thermodynamic properties of synthetic 2M, Muscovite $KAl_2[AlSi_3O_{10}(OH)_2]$: Contributions to Mineralogy and Petrology, v. 48, n. 2, p. 89–114, http://dx.doi.org/10.1007/BF00418612

Chatterjee, N. D., Krüger, R., Haller, G., and Olbricht, W., 1998, The Bayesian approach to an internally consistent thermodynamic database: theory, database, and generation of phase diagrams: Contributions to Mineralogy and Petrology, v. 133, n. 1–2, p. 149–168, http://dx.doi.org/10.1007/s004100050444

Chen, C. H., 1975, A method of estimation of standard free energies of formation of silicate minerals at 298.15°K: American Journal of Science, v. 275, n. 7, p. 801–817, http://dx.doi.org/10.2475/ajs.275.7.801

Chermak, J. A., 1993, Low temperature experimental investigation of the effect of high pH KOH solutions on the Opalinus Shale, Switzerland: Clays and Clay Minerals, v. 41, n. 3, p. 365–372, http://dx.doi.org/10.1346/CCMN.1993.0410313

Chermak, J. A., and Rimstidt, J. D., 1989, Estimating the thermodynamic properties (ΔG°f and ΔH°f) of silicate minerals at 298 K from the sum of polyhedral contributions: American Mineralogist, v. 74, n. 9–10, p. 1023–1031.

Cho, M., Maruyama, S., and Liou, J. G., 1987, An experimental investigation of heulandite-laumontite equilibrium at 1000 to 2000 bar P_{fluid}: Contributions to Mineralogy and Petrology, v. 97, n. 1, p. 43–50, http://dx.doi.org/10.1007/BF00375213

Circone, S., and Navrotsky, A., 1992, Substitution of (super [6,4])Al in phlogopite: high- temperature solution calorimetry, heat capacities, and thermodynamic properties of the phlogopite -eastonite join: American Mineralogist, v. 77, n. 11–12, p. 1191–1205.

Coggon, R., and Holland, T. J. B., 2002, Mixing properties of phengitic micas and revised garnet-phengite thermobarometers: Journal of Metamorphic Geology, v. 20, n. 7, p. 683–696, http://dx.doi.org/10.1046/j.1525-1314.2002.00395.x

Coombs, D. S., Alberti, A., Armbruster, T., Artioli, G., Colella, C., Galli, E., Grice, J. D., Liebau, F., Minato, H., Nickel, E. H., Passaglia, E., Peacor, D. R., Quartieri, S., Rinaldi, R., Ross, M., Sheppard, R. A., Tillmanns, E., and Vezzalini, G., 1997, Recommended nomenclature for zeolite minerals: Report of the subcommittee on zeolites of the International Mineralogical Association, Commission on New Minerals and Mineral Names: Canadian Mineralogist, v. 35, n. 6, p. 1571–1606.

Cox, J. D., Wagman, D. D., and Medvedev, V. A., 1989, CODATA key values for thermodynamics: New York, Hemisphere Publishing Corporation, 271 p.

Dachs, E., and Benisek, A., 1995, The stability of annite+quartz: reversed experimental data for the reaction 2 annite+3 quartz = 2 sanidine+3 fayalite +2 H_2O: Contributions to Mineralogy and Petrology, v. 121, n. 4, p. 380–387, http://dx.doi.org/10.1007/s004100050103

——— 1997, Annite stability revised: hydrogen-sensor data for the reaction annite = sanidine + magnetite + H_2: additional results and reply to Chou: Contributions to Mineralogy and Petrology, v. 128, n. 2–3, p. 306–311, http://dx.doi.org/10.1007/s004100050311

Donahoe, R. J., Hemingway, B. S., and Liou, J. G., 1990, Thermochemical data for merlinoite. I, Low temperature heat capacities entropies and enthalpies of solutions of 298.15 K of six synthetic samples having various Si/Al and Na/(Na+K) ratios: American Mineralogist, v. 75, n. 1–2, p. 188–200.

Drebushchak, V. A., Naumov, V. N., Nogteva, V. V., Belitsky, I. A., and Paukov, I. E., 2000, Low-temperature heat capacity of heulandite: comparison with clinoptilolite: Thermochimica Acta, v. 348, n. 1–2, p. 33–40, http://dx.doi.org/10.1016/S0040-6031(99)00453-0

Essene, E. J., and Peacor, D. R., 1995, Clay mineral thermometry–A critical perspective: Clays and Clay Minerals, v. 43, n. 5, p. 540–553, http://dx.doi.org/10.1346/CCMN.1995.0430504

Eugster, H. P., Albee, A. L., Bence, A. E., Thompson, J. B., Jr., and Waldbaum, D. R., 1972, The two–phase region and excess mixing properties of Paragonite-Muscovite crystalline solutions: Journal of Petrology, v. 13, n. 1, p. 147–139, http://dx.doi.org/10.1093/petrology/13.1.147

Evans, B. W., 2004, The Serpentinite Multisystem Revisited: Chrysotile Is Metastable: International Geology Review, v. 46, n. 6, p. 479–506, http://dx.doi.org/10.2747/0020-6814.46.6.479

Evans, B. W., and Guggenheim, S., 1988, Talc, Pyrophyllite and related minerals, *in* Bailey, S. W., editor, Hydrous Phyllosilicates (exclusive of the micas): Reviews in Mineralogy and Geochemistry, v. 19, p. 225–294.

Fialips, C. I., Navrotsky, A., and Petit, S., 2001, Crystal properties and energetics of synthetic kaolinite: American Mineralogist, v. 86, n. 3, p. 304–311.

Fridriksson, T., Neuhoff, P. S., Arnórsson, S., and Bird, D. K., 2001, Geological constraints on the thermodynamic properties of the stilbite-stellerite solid solution in low-grade metabasalts: Geochimica et Cosmochimica Acta, v. 65, n. 21, p. 3993–4008, http://dx.doi.org/10.1016/S0016-7037(01)00629-9

Fridriksson, T., Neuhoff, P. S., Viani, B. E., and Bird, D. K., 2004, Experimental determination of thermodynamic properties of ion-exchange in heulandite: Binary ion-exchange experiments at 55 and 85 °C involving Ca^{2+}, Sr^{2+}, Na^{+} and K^{+}: American Journal of Science, v. 304, n. 4, p. 287–332, http://dx.doi.org/10.2475/ajs.304.4.287

Gailhanou, H., 2005, ms, Détermination expérimentale des propriétés thermodynamiques et étude des nanostructures de minéraux argileux: Marseille, France, Université Paul Cézanne Aix-Marseille III, Ph. D. thesis, 262 p.

Gailhanou, H., and Blanc, P., 2009, THERMOCHIMIE: Acquisition de's propriétés thermodynamiques d'une nontronite et d'une beidellite et révision des données de la saponite Sap-Ca-1: Orléans, BRGM.

Gailhanou, H., van Miltenburg, J. C., Rogez, J., Olives, J., Amouric, M., Gaucher, E. C., and Blanc, P., 2007, Thermodynamic properties of anhydrous smectite MX-80, illite IMt-2 and mixed-layer illite-smectite ISCz-1 as determined by calorimetric methods. Part I: Heat capacities, heat contents and entropies: Geochimica et Cosmochimica Acta, v. 71, n. 22, p. 5463–5473, http://dx.doi.org/10.1016/j.gca.2007.09.020

Gailhanou, H., Rogez, J., van Miltenburg, J. C., Van Genderen, A. C. G., Grenèche, M., Gilles, C., Jalabert, D., Michau, N., Gaucher, E. C., and Blanc, P., 2009, Thermodynamic properties of chlorite CCa-2. Heat capacities, heat contents and entropies: Geochimica et Cosmochimica Acta, v. 73, n. 16, p. 4738–4749, http://dx.doi.org/10.1016/j.gca.2009.04.040

Gailhanou, H., Blanc, P., Rogez, J., Mikaelian, G., Kawaji, H., Olives, J., Amouric, M., Denoyel, R., Bourrely, S., Montouillout, V., Vieillard, P., Fialips, C. I., Michau, N., and Gaucher, E. C., 2012, Thermodynamic properties of illite, smectite and beidellite by calorimetric methods: Enthalpies of formation, heat capacities, entropies and Gibbs free energies of formation: Geochimica et Cosmochimica Acta, v. 89, p. 279–301, http://dx.doi.org/10.1016/j.gca.2012.04.048

Gailhanou, H., Blanc, P., Rogez, J., Mikaelian, G., Horiuchi, K., Yamamura, Y., Saito, K., Kawaji, H., Warmont, F., Grenèche, M., Vieillard, P., Fialips, C. I., Giffaut, E., and Gaucher, E. C., 2013, Thermodynamic properties of saponite, nontronite and vermiculite derived from calorimetric measurements: American Mineralogist, v. 98, n. 10, p. 1834–1847, http://dx.doi.org 10.2138/am.2013.4344

Garvin, D., Parker, V. B., White, H. J., and CODATA. Task Group on Chemical Thermodynamic Tables, 1987, CODATA thermodynamic tables: selections for some compounds of calcium and related mixtures: a prototype set of tables: Washington, Hemisphere Publishing Corporation, 356 p.

Gaucher, E. C., and Blanc, P., 2006, Cement/clay interactions - A review: Experiments, natural analogues, and modeling: Waste Management, v. 26, n. 7, p. 776–788, http://dx.doi.org/10.1016/j.wasman.2006.01.027

Gaucher, E. C., Blanc, P., Matray, J.-M., and Michau, N., 2004, Modeling diffusion of an alkaline plume in a clay barrier: Applied Geochemistry, v. 19, n. 10, p. 1505–1515, http://dx.doi.org/10.1016/j.apgeochem.2004.03.007

Giffaut, E., Grivé, M., Blanc, P., Vieillard, P., Colàs, E., Gailhanou, H., Gaboreau, S., Marty, N., Madé, B., and Duro, L., 2014, Andra thermodynamic database for performance assessment: ThermoChimie: Applied Geochemistry, v. 49, p. 225–236, http://dx.doi.org/10.1016/j.apgeochem.2014.05.007

Giret, A., Verdier, O., and Nativel, P., 1992, The zeolitization model of Kerguelen islands, Southern Indian Ocean, *in* Yoshida, Y., Daminuma, K., and Shiraishi, K., editors, Recent Progress in Antarctic Earth Science: Tokyo, Terrapub, p. 457–463.

Gottschalk, M., 1997, Internally consistent thermodynamic data for rock-forming minerals in the system SiO_2-TiO_2-Al_2O_3-Fe_2O_3-CaO-MgO-FeO-K_2O-Na_2O-H_2O-CO_2: European Journal of Mineralogy, v. 9, n. 1, p. 175–223.

Grivé, M., Duro, L., Colàs, E., and Giffaut, E., 2015, Thermodynamic data selection applied to radionuclides and chemotoxic elements: An overview of the ThermoChimie-TDB: Applied Geochemistry, Geochemical Speciation Codes and Databases, v. 55, p. 85–94, http://dx.doi.org/10.1016/j.apgeochem.2014.12.017

Haselton, H. T., Jr., Cygan, G. L., and Jenkins, D. M., 1995, Experimental study of muscovite stability in pure H_2O and 1 molal KCl-HCl solutions: Geochimica et Cosmochimica Acta, v. 59, n. 3, p. 429–442, http://dx.doi.org/10.1016/0016-7037(94)00380-5

Helgeson, H. C., and Aagaard, P., 1985, Activity/composition relations among silicates and aqueous solutions. I. Thermodynamics of intrasite mixing and substitutional order/disorder in minerals: American Journal of Science, v. 285, n. 9, p. 769–844, http://dx.doi.org/10.2475/ajs.285.9.769

Helgeson, H. C., and Mackenzie, F. T., 1970, Silicate sea water equilibria in the ocean system: Deep Sea Research and Oceanographic Abstracts, v. 17, n. 5, http://dx.doi.org/10.1016/0011-7471(70)90005-7
Helgeson, H. C., Delany, J. M., Nesbitt, H. W., and Bird, D. K., 1978, Summary and critique of the thermodynamic properties of the rock-forming minerals: American Journal of Science, v. 278-A, p. 229.
Hemingway, B. S., 1990, Thermodynamic properties for bunsenite, NiO, magnetite, Fe_3O_4, and hematite, Fe_2O_3, with comments on selected oxygen buffer reactions: American Mineralogist v. 75, n. 7–8, p. 781–790.
——— 1991, Thermodynamic properties of Anthophyllite and talc- Corrections and discussion of calorimetric data: American Mineralogist, v. 76, n. 9–10, p. 1589–1596.
Hemingway, B. S., and Robie, R. A., 1977, Enthalpies of formation of low albite ($NaAlSi_3O_8$), gibbsite ($Al(OH)_3$) and $NaAlO_2$; revised values for $\Delta H°_{f,298}$ and $\Delta G°_{f,298}$ of some aluminosilicate minerals: U.S. Geological Survey Journal of Research, v. 5, n. 4, p. 413–429.
——— 1984, Thermodynamic properties of zeolites - low temperature heat capacities and thermodynamic functions for phillipsite and clinoptilolite; estimates of the thermochemical properties of zeolitic water at low temperature: American Mineralogist, v. 69, n. 7–8, p. 692–700.
——— 1990, Heat capacities and thermodynamic properties of annite (aluminous iron biotite): American Mineralogist, v. 75, n. 1–2, p. 183–187.
Hemingway, B. S., Robie, R. A., Kittrick, J. A., Grew, E. S., Nelen, J. A., and London, D., 1984, The heat capacities of osumilite from 298.15 to 1000 K, the thermodynamic properties of two natural chlorites to 500 K, and the thermodynamic properties of petalite to 1800°K: American Mineralogist, 69, n. 7–8, p. 701–710.
Hess, P. C., 1966, Phase equilibria of some minerals in the K_2O-Na_2O-Al_2O_3-SiO_2-H_2O system at 25° and 1 atm.: American Journal of Science, v. 264, n. 4, p. 289–309, http://dx.doi.org/10.2475/ajs.264.4.289
Holland, T. J. B., 1989, Dependence of entropy on volume for silicate and oxide minerals. A review and a predicture model: American Mineralogist, v. 74, n. 1–2, p. 5–13.
Holland, T. J. B., and Powell, R., 1990, An enlarged and updated internally consistent thermodynamic dataset with uncertainties and correlations: the system K_2O-Na_2O-CaO-MgO-MnO-FeO-Fe_2O_3-Al_2O_3-TiO_2-SiO_2-C-H_2-O_2: Journal of Metamorphic Geology, v. 8, n. 1, p. 89–124, http://dx.doi.org/10.1111/j.1525-1314.1990.tb00458.x
——— 1998, An internally consistent thermodynamic data set for phases of petrological interest: Journal of Metamorphic Geology, v. 16, n. 3, p. 309–343, http://dx.doi.org/10.1111/j.1525-1314.1998.00140.x
Holland, T. J. B., Baker, J., and Powell, R., 1998, Mixing properties and activity-composition relationships of chlorites in the system MgO-FeO-Al_2O_3-SiO_2-H_2O: European Journal of Mineralogy, v. 10, n. 3, p. 395–406.
Howell, D. A., Johnson, G. K., Tasker, I. R., and O'Hare, P. A. G., and Wise, W. S., 1990, Thermodynamic properties of the zeolite Stilbite: Zeolites, v. 10, n. 6, p. 525–531, http://dx.doi.org/10.1016/S0144-2449(05)80307-0
Johnson, G. K., Flotow, H. E., and O'Hare, P. A. G., W. S., 1982, Thermodynamic studies of zeolites: analcime and dehydrated analcime: American Mineralogist, v. 67, n. 7–8, p. 736–748.
Johnson, G. K., Flotow, H. E., O'Hare, P. A. G., and Wise, W. S., 1983, Thermodynamic studies of zeolites: natrolite, mesolite and scolecite: American Mineralogist, v. 68, n. 11–12, p. 1134–1145.
——— 1985, Thermodynamic studies of zeolites: heulandite: American Mineralogist, v. 70, n. 9–10, p. 1065–1071.
Johnson, G. K., Tasker, I. R., Jurgens, R., and O'Hare, P. A. G., 1991, Thermodynamic studies of Zeolites-Clinoptilolite: Journal of Chemical Thermodynamics, v. 23, n. 5, p. 475-484, http://dx.doi.org/10.1016/S0021-9614(05)80135-1
Johnson, G. K., Tasker, I. R., Flotow, H. E., O'Hare, P. A. G., and Wise, W. S., 1992, Thermodynamic studies of mordenite, dehydrated mordenite and gibbsite: American Mineralogist, v. 77, n. 1–2, p. 85–93.
Johnson, J. W., Oelkers, E. H., and Helgeson, H. C., 1992, SUPCRT92: A software package for calculating the standard molal thermodynamic properties of minerals, gases, aqueous species and reactions from 1 to 5000 bars and 0 to 1000 °C: Computers and Geosciences, v. 18, n. 7, p. 889–947, http://dx.doi.org/10.1016/0098-3004(92)90029-Q
Kahl, W.-A., and Maresch, W. V., 2001, Enthalpies of formation of tremolite and talc by high-temperature solution calorimetry–a consistent picture: American Mineralogist, v. 86, n. 11–12, p. 1345–1357.
Kashik, S. A., Karpov, I. K., and Kozlova, C. V., 1978, Calculation of the Gibbs free energy of layered silicate by the empirical method: Geokhimiya, v. 3, p. 428–433.
Kiseleva, I., Navrotsky, A., Belitsky, I. A., and Fursenko, B. A., 1996, Thermochemistry and phase equilibria in calcium zeolites: American Mineralogist, v. 81, n. 5–6, p. 658–667.
——— 2001, Thermochemical study of calcium zeolites- heulandite and stilbite: American Mineralogist, v. 86, n. 4, p. 448–455.
Kittrick, J. A., 1984, Solubility measurements of phases in three illites: Clays and Clay Minerals, v. 32, n. 2, p. 115–124, http://dx.doi.org/10.1346/CCMN.1984.0320205
Kittrick, J. A., and Peryea, F. J., 1988, Experimental validation of the monophase structure model for montmorillonite solubility: Soil Science Society of America Journal, v. 52, n. 4, p. 1199–1201, http://dx.doi.org/10.2136/sssaj1988.03615995005200040059x
——— 1989, The monophase model for magnesium-saturated montmorillonite: Soil Science Society of America Journal, v. 53, n. 1, p. 292–295, http://dx.doi.org/10.2136/sssaj1989.03615995005300010053x
Krupka, K. M., Robie, R. A., and Hemingway, B. S., 1979, High-temperature heat capacities of corundum, periclase, anorthite, $CaAl_2Si_2O_8$ glass, muscovite, pyrophyllite, $KAlSi_3O_8$ grossular, and $NaAlSi_3O_8$ glass: American Mineralogist, v. 64, n. 1–2, p. 86–101.
La Iglesia, A., and Félix, J. F., 1994, Estimation of thermodynamic properties of mineral carbonates at high

and low temperatures from the sum of polyhedral contributions: Geochimica et Cosmochimica Acta, v. 58, n. 19, p. 3983–3991, http://dx.doi.org/10.1016/0016-7037(94)90261-5
Liou, J. G., 1971, P-T stabilities of Laumontite, wairakite and lawsonite and related minerals in the system $CaAl_2Si_2O_8$-SiO_2-H2O: Journal of Petrology, v. 12, n. 2, p. 349–411, http://dx.doi.org/10.1093/petrology/12.2.379
Lipsicas, M., Raythatha, R. H., Pinnavaia, T. J., Johnson, I. D., Giese, R. F., Jr., Costanzo, P. M., and Robert, J. L., 1984, Silicon and aluminium site distributions in 2:1 layered silicate clays: Nature, v. 309, p. 604–607, http://dx.doi.org/10.1038/309604a0
Loewenstein, W., 1954, The distribution of aluminum in the tetrahedra of silicates and aluminates: American Mineralogist, v. 39, p. 92–96.
Marty, N. C. M., Tournassat, C., Burnol, A., Giffaut, E., and Gaucher, E. C., 2009, Influence of reaction kinetics and mesh refinement on the numerical modelling of concrete/clay interactions: Journal of Hydrology, v. 364, n. 1–2, p. 58–72, http://dx.doi.org/10.1016/j.jhydrol.2008.10.013
Massonne, H. J., and Szpurka, Z., 1997, Thermodynamic properties of white micas on the basis of high-pressure experiments in the systems K_2O-MgO-Al_2O_3-SiO_2-H_2O and K_2O-FeO-Al_2O_3-SiO_2-H_2O: Lithos, v. 41, n. 1–3, p. 229–250, http://dx.doi.org/10.1016/S0024-4937(97)82014-2
Mattigod, S. V., and Sposito, G., 1978, Improved method for estimating the standard free energies of formation ($\Delta G^\circ_{f\ 298.15}$) of smectites: Geochimica et Cosmochimica Acta, v. 42, n. 12, p. 1753–1762, http://dx.doi.org/10.1016/0016-7037(78)90232-6
May, H. M., Kinniburgh, D. G., Helmke, P. A., and Jackson, M. L., 1986, Aqueous dissolution, solubilities and thermodynamic stabilities of common aluminosilicate clay minerals: Kaolinite and smectites: Geochimica et Cosmochimica Acta, v. 50, n. 8, p. 1667–1677, http://dx.doi.org/10.1016/0016-7037(86)90129-8
McPhail, D. C., Berman, R. G., and Greenwood, H. J., 1990, Experimental and theoretical constraints on aluminum substitution in magnesian chlorite, and a thermodynamic model for H_2O in magnesian cordierite: The Canadian Mineralogist, v. 28, p. 859–874.
Mercury, L., Vieillard, P., and Tardy, Y., 2001, Thermodynamics of Ice polymorphs and "Ice-like" water in hydrates and hydroxides: Applied Geochemistry, v. 16, n. 2, p. 161–181, http://dx.doi.org/10.1016/S0883-2927(00)00025-1
Miyano, T., and Klein, C., 1983, Phase relations of orthopyroxene, olivine and grunerite in high grade metamorphic iron formation: American Mineralogist, v. 68, n. 7–8, p. 699–716.
Mosser-Ruck, R., Cathelineau, M., Guillaume, D., Charpentier, D., Rousset, D., Barres, O., and Michau, N., 2010, Effects of temperature, pH, and iron/clay and liquid/clay ratios on Experimental Conversion of Dioctahedral Smectite To Berthierine, Chlorite, Vermiculite or Saponite: Clays and Clay Minerals, v. 58, n. 2, p. 280–291, http://dx.doi.org/10.1346/CCMN.2010.0580212
Murphy, W. M., Pabalan, R. T., Prikryl, J. D., and Goulet, C. J., 1996, Reaction kinetics and thermodynamics of aqueous dissolution and growth of analcime and Na-clinoptilolite at 25 degrees C: American Journal of Science, v. 296, n. 2, p. 128–186, http://dx.doi.org/10.2475/ajs.296.2.128
Neuhoff, P. S., and Wang, J., 2007, Heat capacity of hydration in zeolites: American Mineralogist, v. 92, n. 8–9, p. 1358–1367, http://dx.doi.org/10.2138/am.2007.2537
Neuhoff, P. S., Hovis, G. L., Balassone, G., and Stebbins, J. F., 2004, Thermodynamic properties of analcime solid solutions: American Journal of Science, v. 304, n. 1, p. 21–66, http://dx.doi.org/10.2475/ajs.304.1.21
Nriagu, J. O., 1975, Thermochemical approximation for clay minerals: American Mineralogist, v. 60, n. 9–10. p. 834–839.
Ogorodova, L. P., Mel'chakova, L. V., Kiseleva, I. A., Shuriga, T. N., and Kononov, O. V., 2009, The enthalpy of formation of natural siderophyllite: Russian Journal of Physical Chemistry A, v. 83, n. 3, p. 346–349, http://dx.doi.org/10.1134/S0036024409030042
Ogorodova, L. P., Kiseleva, I. A., and Mel'chakova, L. V., 2010, Thermodynamic properties of lithium micas: Geochemistry International, v. 48, n. 4, p. 415–418, http://dx.doi.org/10.1134/S0016702910040117
Ogorodova, L. P., Kiseleva, I. A., Melchakova, L. V., Vigasina, M. F., and Vladykin, N. V., 2012, Calorimetric measurement of the enthalpy of formation, dehydration, and dehydroxylation of vermiculite: Geochemistry International, v. 50, n. 10, p. 878–883, http://dx.doi.org/10.1134/S001670291208006X
Parker, V. B., and Khodakovskii, I. L., 1995, Thermodynamic Properties of the Aqueous Ions (2+ and 3+) of Iron and the Key Compounds of Iron: Journal of Physical and Chemical Reference Data, v. 24, p. 1699–1745, http://dx.doi.org/10.1063/1.555964
Parra, T., Vidal, O., and Agard, P., 2002, A thermodynamic model for Fe-Mg dioctahedral K white micas using data from phase-equilibrium experiments and natural pelitic assemblages: Contributions to Mineralogy and Petrology, v. 143, n. 6, p. 706–732, http://dx.doi.org/10.1007/s00410-002-0373-6
Parra, T., Vidal, O., and Theye, T., 2005, Experimental data on the Tschermak substitution in Fe-chlorite: American Mineralogist, v. 90, n. 2–3, p. 359–370, http://dx.doi.org/10.2138/am.2005.1556
Paukov, I. E., and Fursenko, B. A., 1998, Low-temperature heat capacity and thermodynamic functions of laumontite: Geokhimiya, v. 12, p. 1301–1303.
Pauling, L., 1960, The nature of the chemical bond: New York, Cornell University Press, 3rd edition, 430 p.
Pokrovskii, V. A., and Helgeson, H. C., 1995, Thermodynamic properties of aqueous species and the solubilities of minerals at high pressures and temperatures; the system Al_2O_3-H_2O-NaCl: American Journal of Science, v. 295, n. 10, p. 1255–1342, http://dx.doi.org/10.2475/ajs.295.10.1255
Rasmussen, M. G., Evans, B. W., and Kuehner, S. M., 1998, Low-temperature fayalite, greenalite, and minnesotaite from the Overlook gold deposit, Washington: Phase relations in the system FeO-SiO_2-H_2O: The Canadian Mineralogist, v. 36, n. 1, p. 147–162.
Reesman, A. L., and Keller, W. D., 1968, Aqueous solubility studies of high-alumina and clay minerals: American Mineralogist, v. 53, n. 5–6, p. 929–942.
Richet, P., Bottinga, Y., Denielou, L., Petitet, J. P., and Tequi, C., 1982, Thermodynamic properties of quartz,

cristobalite and amorphous SiO_2: drop calorimetry measurements between 1000 and 1800 K and a review from 0 to 2000 K: Geochimica et Cosmochimica Acta, v. 46, n. 12, p. 2639–2658, http://dx.doi.org/10.1016/0016-7037(82)90383-0

Robie, R. A., and Hemingway, B. S., 1984, Heat capacities and entropies of phlogopite ($KMg3[AlSi3O_{1O}](OH)_2$) and paragonite ($NaAl_2[AlSi_3O_{1O}](OH)_2$) between 5 and 9OO K and estimates of the enthalpies and Gibbs free energies of formation: American Mineralogist, v. 69, n. 9–10, p. 858–868.

——— 1991, Heat capacities of kaolinite from 7° to 380°K and of DMSO-intercalated kaolinite from 20 to 310°K. The entropy of kaolinite $Al_2Si_2O_5(OH)_4$: Clays and Clay Minerals, v. 4, p. 362–368, http://dx.doi.org/10.1346/CCMN.1991.0390404

——— 1995, Thermodynamic properties of minerals and Related Substances at 298.15 K and 1 bar (10^5 Pascals) pressure and higher temperatures: U.S. Geological Survey Bulletin, v. 2131, 461 p.

Robie, R. A., and Stout, J. W., 1963, Heat capacity from 12 to 3O5 °K and entropy of talc and tremolite: The Journal of Physical Chemistry, v. 67, n. 11, p. 2252–2256, http://dx.doi.org/10.1021/j100805a003

Robie, R. A., Hemingway, B. S., and Wilson, W. H., 1976, The heat capacities of calorimetry conference copper and of muscovite $KAl_2(AlSi_3)O_{10}(OH)_2$, pyrophyllite $Al_2Si_4O_{10}(OH)_2$, and illite $K_3(Al_7Mg)(Si_{14}Al_2)O_{40}(OH)_8$ between 15 and 375 K and their standard entropies at 298.15 K.: U.S. Geological Survey Journal of Research, v. 4, p. 631–644.

Robinson, G. R., and Haas, J. L., 1983, Heat capacity, relative enthalpy and calorimetric entropy of silicate minerals: an empirical method of prediction: American Mineralogist, v. 68, n. 5–6, p. 541–553.

Robinson, G. R., Haas, J. L., Jr., Schafer, C. M., and Haselton, H. T., Jr., 1982, Thermodynamic and thermophysical properties of selected phases in the MgO-SiO_2-H_2O-CO_2, CaO-Al_2O_3-SiO_2-H_2O-CO_2, and Fe-FeO-Fe_2O_3-SiO_2 chemical systems, with special emphasis on the properties of basalts and their mineral components: U.S. Geological Survey Open-file Report, v. 83–79, 429 p.

Roux, J., and Hovis, G. L., 1996, Thermodynamic mixing models for muscovite-paragonite solutions based on solution calorimetric and phase equilibrium data: Journal of Petrology, v. 37, n. 5, p. 1241–1254, http://dx.doi.org/10.1093/petrology/37.5.1241

Roy, R., and Romo, L. A., 1957, Weathering studies. 1. New data on Vermiculite: Journal of Geology, v. 65, n. 6, p. 603–610, http://dx.doi.org/10.1086/626466

Saccocia, P. J., and Seyfried, W. E., 1993, A Resolution of Discrepant Thermodynamic Properties for Chamosite Retrieved from Experimental and Empirical Techniques: American Mineralogist, v. 78, n. 5–6, p. 607–611.

——— 1994, The Solubility of Chlorite Solid Solutions in 3.2 Wt% NaCl Fluids from 300-400 °C, 500 Bars: Geochimica et Cosmochimica Acta, v. 58, n. 2, p. 567–585, http://dx.doi.org/10.1016/0016-7037(94)90489-8

Sanz, J., and Serratosa, J. M., 1984, Silicon-29 and aluminum-27 high-resolution MAS-NMR spectra of phyllosilicates: Journal of the American Chemical Society, v. 106, n. 17, p. 4790–4793, http://dx.doi.org/10.1021/ja00329a024

Shibue, Y., 1981, Cation-exchange reactions of siliceous and aluminous phillipsites: Clays and Clay Minerals, v. 29, n. 5, p. 397–402, http://dx.doi.org/10.1346/CCMN.1981.029050C

Shim, S. H., Navrotsky, A., Gaffney, T. R., and Macdougall, J. E., 1999, Chabazite: Energetics of hydration, enthalpy of formation, and effect of cations on stability: American Mineralogist, v. 84, n. 11–12, p. 1870–1882.

Sposito, G., 1986, The polymer model of thermochemical clay mineral stability: Clays and Clay Minerals, v. 34, n. 2, p. 198–203, http://dx.doi.org/10.1346/CCMN.1986.0340210

Stoessell, R. K., 1979, A regular solution site mixing model for illites: Geochimica et Cosmochimica et Acta, v. 43, n. 8, p. 1151–1159, http://dx.doi.org/10.1016/0016-7037(79)90108-X

——— 1981, Refinements in a site-mixing model for illites: local electrostatic balance and the quasi-chemical approximation: Geochimica et Cosmochimica Acta, v. 45, n. 10, p. 1733–1741, http://dx.doi.org/10.1016/0016-7037(81)90007-7

——— 1984, Regular solution site mixing model for chlorites: Clays and Clay Minerals, v. 32, n. 3, p. 205–212.

——— 1988, 25 °C and 1 atm dissolution experiments of sepiolite and kerolite: Geochimica et Cosmochimica Acta, v. 52, n. 2, p. 365–374, http://dx.doi.org/10.1016/0016-7037(88)90092-0

Sverjensky, D. A., 1985, The distribution of divalent trace elements between sulfides, oxides, silicates and hydrothermal solutions: I. Thermodynamic basis: Geochimica et Cosmochimica Acta, v. 49, n. 3, p. 853–864, http://dx.doi.org/10.1016/0016-7037(85)90177-2

Sverjensky, D. A., and Molling, P. A., 1992, A linear free energy relationship for crystalline solids and aqueous ions: Nature, v. 356, p. 231–234, http://dx.doi.org/10.1038/356231a0

Tardy, Y., and Duplay, J., 1992, A method of estimating the Gibbs free energies of formation of hydrated and dehydrated clays minerals: Geochimica et Cosmochimica Acta, v. 56, n. 8, p. 3007–3029, http://dx.doi.org/10.1016/0016-7037(92)90287-S

Tardy, Y., and Fritz, B., 1981, An ideal solid solution model for calculating solubility of clay minerals: Clays and Clay minerals, v. 16, p. 361–373, http://dx.doi.org/10.1180/claymin.1981.016.4.05

Tardy, Y., and Garrels, R. M., 1974, A method of estimating the Gibbs energies of formation of layer silicates: Geochimica et Cosmochimica Acta, v. 38, n. 7, p. 1101–1116, http://dx.doi.org/10.1016/0016-7037(74)90007-6

Tutolo, B. M., Kong, X-Z, Seyfried, W. E., Jr., and Saar, M. O., 2014, Internal consistency in aqueous geochemical data revisited: Applications to the aluminum system: Geochimica et Cosmochimica Acta, v. 133, p. 216–234, http://dx.doi.org/10.1016/j.gca.2014.02.036

Ulbrich, H. H., and Waldbaum, D. R., 1976, Structural and other contributions to the third-law entropies of silicates: Geochimica et Cosmochimica Acta, v. 40, n. 1, p. 1–24, http://dx.doi.org/10.1016/0016-7037(76)90189-7

Van Hinsberg, V. J., Vriend, S. P., and Schumacher, J. C., 2005a, A new method to calculate end-member thermodynamic properties of minerals from their constituent polyhedra I: enthalpy, entropy and molar volume: Journal of Metamorphic Geology, v. 23, n. 3, p. 165–179, http://dx.doi.org/10.1111/j.1525-1314.2005.00569.x

——— 2005b, A new method to calculate end-member thermodynamic properties of minerals from their constituent polyhedra II: heat capacity, compressibility and thermal expansion: Journal of Metamorphic Geology, v. 23, n. 8, p. 681–693, http://dx.doi.org/10.1111/j.1525-1314.2005.00603.x

Varadachari, C., Kudrat, M., and Ghosh, K., 1994, Evaluation of standard free energies of formation of clay minerals by an improved regression method: Clays and Clay Minerals, v. 42, n. 3, p. 298–307, http://dx.doi.org/10.1346/CCMN.1994.0420308

Velde, B., 1977, Clays and Clay Minerals in Natural and Synthetic systems: Developments in Sedimentology, v. 21, p. 1–218.

Vidal, O., and Dubacq, B., 2009, Thermodynamic modelling of clay dehydration, stability and compositional evolution with temperature, pressure and H_2O activity: Geochimica et Cosmochimica Acta, v. 73, n. 21, p. 6544–6564, http://dx.doi.org/10.1016/j.gca.2009.07.035

Vidal, O., Parra, T., and Trotet, F., 2001, A thermodynamic model for Fe-Mg aluminous chlorite using data from phase equilibrium experiments and natural pelitic assemblages in the 100 ° to 600 °C and 1 to 25 kB range: American Journal of Science, v. 301, n. 6, p. 557–592, http://dx.doi.org/10.2475/ajs.301.6.557

Vidal, O., Parra, T., and Vieillard, P., 2005, Thermodynamic properties of the Tschermak solid solution in Fe-chlorite: Application to natural examples and possible role of oxidation: American Mineralogist, v. 90, n. 2–3, p. 347–358, http://dx.doi.org/10.2138/am.2005.1554

Vieillard, P., 1994a, Prediction of enthalpy of formation based on refined crystal structures of multisite compounds: Part 1. Theories and examples: Geochimica et Cosmochimica Acta, v. 58, n. 19, p. 4049–4063, http://dx.doi.org/10.1016/0016-7037(94)90266-6

——— 1994b, Prediction of enthalpy of formation based on refined crystal structures of multisite compounds: Part 2. Application to minerals belonging to the system Li_2O-Na_2O-K_2O-BeO-MgO-CaO-MnO-FeO-Fe_2O_3-Al_2O_3-SiO_2-H_2O. Results and discussion: Geochimica et Cosmochimica Acta, v. 58, n. 19, p. 4065–4107, http://dx.doi.org/10.1016/0016-7037(94)90267-4

——— 2000, A new method for the prediction of Gibbs free energies of formation of hydrated clay minerals based on the electronegativity scale: Clays and Clay Minerals, v. 48, n. 4, p. 459–473, http://dx.doi.org/10.1346/CCMN.2000.0480406

——— 2002, A new method for the prediction of Gibbs free energies of formation of phyllosilicates (10Å and 14Å) based on the electronegativity scale: Clays and Clay Minerals, v. 50, n. 3, p. 352–363, http://dx.doi.org/10.1346/00098600260358120

——— 2010, A predictive model for the entropies and heat capacities of zeolites: European Journal of Mineralogy, v. 22, n. 6, p. 823–836, http://dx.doi.org/10.1127/0935-1221/2010/0022-2026

Vieillard, P., and Tardy, Y., 1988a, Estimation of enthalpies of formation of minerals based on their refined crystal structures: American Journal of Science, v. 288, n. 10, p. 997–1040, http://dx.doi.org/10.2475/ajs.288.10.997

——— 1988b, Une nouvelle échelle d'électronégativité des ions dans les cristaux. Principe et méthode de calcul: Comptes Rendus Académie des Sciences, Paris, v. 306, p. 423–428.

——— 1989, Une nouvelle échelle d'électronégativité des ions dans les oxydes et les hydroxydes: Comptes Rendus Académie des Sciences, Paris, v. 308, p. 1539–1545.

Vieillard, P., Blanc, P., Fialips, C. I., Gailhanou, H., and Gaboreau, S., 2011, Hydration thermodynamics of the SWy-1 montmorillonite saturated with alkali and alkaline-earth cations: a predictive model: Geochimica et Cosmochimica Acta, v. 75, n. 19, p. 5664–5685, http://dx.doi.org/10.1016/j.gca.2011.07.014

Walshe, J. L., 1986, A six component chlorite solid solution model and the conditions of chlorite formation in hydrothermal and geothermal systems: Economic Geology, v. 81, n. 3, p. 681–703, http://dx.doi.org/10.2113/gsecongeo.81.3.681

Weaver, J. S., and Pollard, L. D., 1973, The Chemistry of Clay Minerals: Developments in Sedimentology, v. 15, 213 p.

Whitney, G., 1983, Hydrothermal reactivity of saponite: Clays and Clay Minerals, v. 31, p. 1–8, http://dx.doi.org/10.1346/CCMN.1983.0310101

Wilkin, R. T., and Barnes, H. L., 1998, Solubility and stability of zeolites in aqueous solution: I. Analcime, Na-, and K-clinoptilolite: American Mineralogist, v. 83, n. 7–8, p. 746–761.

Wilson, J., Cressey, G., Cressey, B., Cuadros, J., Ragnarsdottir, K. V., Savage, D., and Shibata, M., 2006, The effect of iron on montmorillonite stability. (II) Experimental investigation: Geochimica et Cosmochimica Acta, v. 70, n. 2, p. 323–336, http://dx.doi.org/10.1016/j.gca.2005.09.023

Yang, S., Navrotsky, A., and Wilkin, R., 2001, Thermodynamics of ion-exchanged and natural clinoptilolite: American Mineralogist, v. 86, n. 4, p. 438–447.

Zeng, Y., and Liou, J. G., 1982, Experimental investigation of yugawaralite-wairakite equilibrium: American Mineralogist, v. 67, n. 9–10, p. 937–943.

Zuyev, V. V., 1987, Effects of cation electronegativity differences in the enthalpies of formation of compound crystals from oxides: Geochemistry International, v. 24, p. 91–100.